

<https://doi.org/10.18524/1810-4215.2025.38.340398>

## A PERSPECTIVE ON ECLIPSING BINARY STAR STUDIES IN THE POST-GAIA ERA

E. F. Milone

University of Calgary, Canada

**ABSTRACT.** Eclipsing binary stars have intrigued astronomers for centuries. To study them is to journey through discoveries and innovations. One of the earliest significant insights came in 1783 when 18-year-old John Goodricke boldly proposed that the periodic dimming of the star Algol, which he and his friend and mentor Edward Pigott had carefully studied, was due to an eclipse by a large dark body revolving about Algol. The communication so impressed the Royal Society of London that Goodricke was awarded the prestigious Copley medal that same year. As observational techniques evolved and photographic photometry developed, the quality as well as the quantity of data increased and by the early 20<sup>th</sup> century, gravitational physics had matured sufficiently that Henry Norris Russell and Harlow Shapley could provide quantitative procedures for finding the properties of stars in eclipsing systems to capitalize on them, an example of a path characterized by Russell (1948) as the Royal Road of Eclipses. Over the following decades, deeper understanding of the physics governing systems of short-period binary stars led to more sophisticated treatments. Zdeněk Kopal and other researchers expanded the analytical framework and initiated more rigorous studies of the internal and orbital dynamics of these systems. The advent of high-speed computing in the 1970s revolutionized the field by enabling simulations of increasing complexity. Continued computational and analytical improvements, coupled with the explosive growth in observational data from wide-field surveys culminating in the Gaia mission, are propelling eclipsing binary research into a new era. We have now both the computational power and the observational depth to probe stellar structure and evolution with unprecedented precision. This presentation highlights key milestones in the study of eclipsing binaries, innovative capabilities in data acquisition and modeling, and the promising role of high-precision infrared photometry. Particular attention will be paid to the enhanced precision attainable through the use of improved passbands for ground-based infrared photometry at local observatories, and to the extended functionalities of the Wilson-Devinney modeling framework, and complementary analytical tools and programs.

**Keywords:** binary stars, eclipsing binaries, photometry, Wilson-Devinney models and program, Gaia, TESS, IRWG passbands.

**АНОТАЦІЯ.** Затемніовані подвійні зорі інтригували астрономів упродовж століть. Їх вивчення – це подорож шляхом відкриттів та інновацій. Одне з перших значних прозрінь сталося в 1783 році, коли 18-річний Джон Гудрайк сміливо припустив, що періодичне ослаблення близьку зорі Алголь, яку він і його друг і наставник Едвард Піготт ретельно вивчали, викликано затемненням темним великим тілом, що обертається навколо Алголю. Це повідомлення настільки вразило Лондонське королівське товариство, що того ж року Гудрайк був нагороджений престижною медаллю Каплі. У міру розвитку методів спостережень та розвитку фотографічної фотометрії якість і кількість даних зростали, і до початку ХХ століття гравітаційна фізика досягла достатньої зрілості, щоб Генрі Норріс Рассел і Харлоу Шеплі змогли запропонувати кількісні процедури для визначення властивостей зір у затемнених системах і отримати з них вигоду, – приклад шляху, який Рассел (1948) охарактеризував як Королівську дорогу затемнень. У наступні десятиліття глибше розуміння фізичних процесів, управлюючих системами короткоперіодичних подвійних зір, привело до появи складніших методів дослідження. Зденек Копал та інші дослідники розширили аналітичні рамки та ініціювали суворіші дослідження внутрішньої та орбітальної динаміки цих систем. Поява високошвидкісних обчислень у 1970-х роках справила революцію у цій галузі, дозволивши проводити моделювання дедалі більшої складності. Удосконалення обчислювальних та аналітичних технологій, що триває, у поєднанні зі стрімким зростанням обсягу спостережних даних, отриманих у ході широкосмугових оглядів, кульмінацією яких стала місяця Gaia, виводять дослідження затемніваних подвійних зір на новий рівень. Тепер у нас є як обчислювальна потужність, так і глибина спостережень, що дозволяють досліджувати структуру та еволюцію зір із безпредентною точністю. У цій презентації висвітлюються ключові віхи у вивченні затемніваних подвійних зір, інноваційні можливості збору даних та моделювання, а також перспективна роль високоточної інфрачервоної фотометрії. Особливу увагу приділено підвищенню точності, яка досягається за рахунок використання покращених смуг пропускання для наземної інфрачервоної фотометрії в місцевих обсерваторіях, а також розширенням функціональним можливостям моделі Вілсона-Девінні

та додатковим аналітичним інструментам та програмам.

**Ключові слова:** подвійні зорі, затемнювані подвійні зорі, фотометрія, моделі та програма Вілсона-Девінні, Gaia, TESS, смуги пропускання IRWG.

## 1. Introduction

One may ask why, after centuries of study, we should continue to observe and analyze binary stars. One may answer: there are many of them! More than half of all stars are in binary or multiple orbital systems. And there are many other reasons! The Earth and every living thing on it depends fundamentally on our local star and the conditions around it, so we should find out a lot about stars. That means getting fundamental data such as the sizes, masses, luminosities (involving sizes and temperatures), distances, and ages of the stars to find how they change over time and why. Such changes result in different positions on color-magnitude diagrams, on isochrone plots, and on evolutionary tracks. Additionally, we would like to observe and to explore the evolution of interacting components. These include stellar wind buffeted or magnetically coupled components as in hot, massive binaries, or cooler RS CVn systems, respectively, or stars undergoing common envelope evolution, or those undergoing mass exchange at varying rates from semi-detached binaries to over-contact W UMa systems to cataclysmic variables and various types of nova-like variables to type Ia supernovae. And then there are the merger products such as blue stragglers (stars in clusters that are too bright and blue, for their positions on plots of luminosity vs. temperature or color), and which, when found in eclipsing systems in globular clusters, may provide clues of ancient hierarchical systems. Finally there are binary systems involving brown dwarfs, white dwarfs, neutron stars, and black holes in various combinations. Milone (2003) provides more details of the contributions to astrophysics of observations of binary stars, anticipated especially from the Gaia mission; that mission did not disappoint; El-Badry (2024) describes the resulting “binary star renaissance.”

A unique contribution of *eclipsing* binary stars is the information gotten by monitoring one star scanning the surface of the other, yielding not only the radii from the precise timings of the four contacts of a total eclipse, but also the limb-darkening resulting from the star’s opacity and temperature profiles, gravity brightening related to the tidal elongation, and active region phenomena such as spots, faculae, and prominences. Additionally, information about other components may be seen in changes in the timing of the eclipses and in measurements of 3<sup>rd</sup> light. These key contributions require highly precise photometric observations. A bonus is their usefulness as potential standard candles (once fully characterized) or, rather, non-standard distance indicators, as each binary system is unique so a derived distance for it does not depend on statistical correlations such as the period-

luminosity relations for Cepheids. It does depend on accurate standardization and flux calibration, and distances from eclipsing binaries can be compared with direct parallax measurements, available now from the Gaia mission in unprecedented numbers. Finally, eclipsing variables self-advertise and are not hard to find: Gaia DR3 lists 2,184,447 eclipsing binaries (Mowlavi et al., 2023), about 20% of all variable objects found thus far in the mission.

The study of eclipsing binary stars is divisible into observational and analytical components, both historically and functionally. A model to be used in the analyses must be physically accurate in order to extract the most precise and accurate elements of the system. The historical trend is toward more exacting data acquisition and reduction techniques, models ever more faithful to the actual physical circumstances of the stars and their systems, and comprehensive analyses that make use of all, while prioritizing the most precise and reliable, information through careful weighting of each datum. Consequently, the growth of understanding of binaries, and stars generally, is inextricably linked to the development of observational equipment and techniques to achieve higher observational precision and accuracy, and to the development of models that incorporate accurate physics and analytical techniques. We begin by reviewing the history of binary star studies and that of eclipsing systems in particular, in the course of which we will examine test cases from two different epochs that illustrate these points.

## 2. Discoveries, Hypotheses, and Observations

By 1750 dozens of pairs of visual double stars had been discovered. From the frequency distribution of angular separations across the sky, J. Michell (1767) argued that “...it is highly probable, and next to a certainty in general, that such double stars ... do really consist of stars placed nearly together, and under the instance of some general law...”. Initially skeptical, William Herschel (1803, p. 340) undertook a thorough investigation of the claim:

“We have already shewn the possibility that two stars, whatsoever be their relative magnitudes, may revolve, either in circles or ellipses, round their common centre of gravity; and that, among the multitude of the stars of the heavens, there should be many sufficiently near each other to occasion this mutual revolution, must also appear highly probable. But neither of these considerations can be admitted in proof of the actual existence of such binary combinations. I shall therefore now proceed to give an account of a series of observations on double stars, comprehending a period of about 25 years, which, if I am not mistaken, will go to prove, that many of them are not merely double in appearance, but must be allowed to be real binary combinations of two stars, intimately held together by the bond of mutual attraction.”

And he did so.

We have already noted the 18<sup>th</sup> century origin of the eclipsing hypothesis for Algol but names given to it in antiquity (*al ghul, Rosha ha Satan, Caput Gorgonis*) suggest that its variability had been noticed for millennia. The first attempt to measure radial velocities of stars based on Doppler's (1842) discovery of the effect on perceived frequency in relative motion was by W. Huggins (1868) who discussed in detail his estimation of the difference between a strong hydrogen line in the spectrum of Sirius and a superimposed bright line from a lamp. He attempted a challenging experiment and provided complete details of how he did it, enabling others to improve on it. The orbital motion of Algol's stars, confirming the eclipse hypothesis, was established first by H. C. Vogel (1890), who thus inaugurated the study of spectroscopic binary stars.

### 2.1. Early observations

Observationally, stellar brightness assessment began with visual estimates by eye with or without telescopic aid. Thus did Goodricke and Piggott determine the period of Algol's variation. This and their subsequent study of  $\beta$  Lyrae effectively marked the onset of eclipsing binary photometry. We leave for another discussion the discoveries of variation of  $\delta$  Cephei and  $\eta$  Aquilae; but altogether the discoveries effectively initiated variable star photometry.

Visual estimates of the relative brightness of stars had been made since ancient times, as in Ptolemy's Almagest star catalog, where "magnitudes" (literally, "sizes") were assigned to stars within constellations and asterisms alongside a description of where the stars lay among the depictions on a celestial sphere. Thus, Algol is described as the "bright one," #12, of stars 12-15 in the Gorgon head. The brightest star in a constellation could be assigned a brightness different than 1, suggesting a roughly uniform scale across the sky. Thus Sirius =  $\alpha$  Canis Majoris is of magnitude " $<1$ " whereas both  $\alpha$  and  $\beta$  Persei (present day designations) are of magnitude 2, and  $\alpha$  and  $\beta$  Lyrae are of magnitude 1 and 3, respectively. Estimates of fractions of visual magnitudes were carried out within brightness sequences of stars by observers such as William Herschel and his son John in the late 17<sup>th</sup>-mid 18<sup>th</sup> centuries. Following attempts by other astronomers to establish a magnitude scale, Norman Pogson (1856) proposed a logarithmic scale in which stars differing by a factor of 100 in brightness were defined to have a magnitude difference of exactly 5 magnitudes. This scale became widely adopted, and later was applied to the light limited to specific regions of the spectrum by the use of spectral filters and detector sensitivities, among other factors, defining the spectral passbands. Examples are the photographic and photo-visual passbands, and the V and B Johnson passbands. The magnitudes in every passband have a zero point which needs to be determined, in order to establish a standard photometric system, to which all observations should be reduced to provide common

understanding of the results. Drilling and Landolt (2000) cite the flux calibrations for a star of zero magnitude and spectral class A0 V (i.e., a white color, and where "V" stands for the luminosity class of a main sequence star) in five Johnson passbands; for example, that for the Johnson B is  $6.40 \cdot 10^{-9}$  erg cm<sup>-2</sup> s<sup>-1</sup> Å<sup>-1</sup>.

Relative brightness measurements systematically began in the 18<sup>th</sup> century. Working with Anders Celsius, Andreas Tulenius (1740) moved a wedge of increasing optical density in an eyepiece to dim a star's light systematically until it disappeared; the distance moved correlated with the brightness of the star. This was the first of a series of extinction-photometry techniques, to be followed by brightness measurements relative to artificial light sources, dimmed by measured amounts of increasing optical density within a movable wedge, or by use of a polarizing prism and rotated analyzer. Procedures like these were carried out widely, but usually yielded precision no better than ~5%. A turning point came with the use of another star as the comparison source. The history of these devices is reviewed by multiple authors writing in Milone & Sterken (2011), starting with Sterken et al. (2011).

### 2.2. Advancing differential photometry: visual vs. photographic photometry

Beginning at the Harvard College and later at the Princeton University Observatory visual comparative devices permitted the observer to vary the brightness of a selected comparison star to visually match the brightness of the target variable star. Working with the Princeton Polarizing Photometer, Russell and associates achieved relatively high precision. John Merrill, for example, achieved a best precision of ~2% observing eclipsing variables RT Lac and RW Com. This exceeded the typical 4-5% best precision obtained from most photographic plate estimates, and a bit better than those obtained from plate measuring engines such as those designed and constructed by H. T. Stetson (1916), and independently by J. Schilt (1922). See Sterken et al. (2011) for a history of these engines. Some photographic techniques made use of joggle plates (producing square images of stars) or extra-focal images, to spread out the light so as to involve more grains on the plate surfaces and improve measurement precision. These could be accommodated by varying the iris aperture of the measuring engines.

**2.2.1. A Case Study of SZ Camelopardalis.** One of the better results from photographic photometry stemmed from a project suggested by Ejnar Herzsprung to A. J. Wesselink, (1941), to compare the brightness of the eclipsing variable SZ Cam (HR 1260, ADS 2984B) with its equally bright visual binary companion (ADS 2984A), 18 arc-sec to the south. A further idea was to use an objective grating to provide multiple images of known brightness ratios of both stars on each exposed plate. He and colleagues obtained 367 plates containing 12,479 useful exposures of the two stars and measured the images with the Schilt photometer. In the systematic determination of the errors at each step,

Wesselink was meticulous in every detail. The study yielded an internal mean precision of  $\sim 2\%$  in the star image measures, the dominant source of internal errors. We discuss the analysis of this work in Section 3.1.1.

### 2.3. Light curve acquisition in the photoelectric and CCD eras

With the advent of the photoelectric cell, photoelectric photometry (PEP) became an alternative method to photography for recording the light of single objects or for scanning small areas of the sky sequentially. Butler and Elliott (1993) describe the pioneering work in the 19<sup>th</sup> century. With a photoconductive selenium cell, Stebbins (1910) achieved 2% precision in recording the light curve of Algol, sufficient to reveal the very shallow secondary minimum in blue light. Whitford (1932) designed and built a DC amplifier to boost the weak current from those devices, increasing the number of observable targets, and proceeded to obtain a light curve of the prototypical short-period eclipsing binary W UMa. John Hall (1934) obtained the earliest near-infrared stellar observations with the aid of a dry ice cooling chamber around the detector housing. With the appearance of the photomultiplier tube (Whitford & Kron, 1937), sensitivity and precision improved again. The original techniques involved measurement of minute currents and voltages; photon counting was a further development that facilitated data collection and provided excellent measurement precision (cf. Armbruster et al., 2011).

Differential photometry with a single detection element involving alternate observation of variable star and comparison and check stars became the normal procedure through the middle of the 20<sup>th</sup> century. However, strict photometric conditions were required for such work and this made observing in many observing sites challenging. Although dry, clear, high-elevation sites are always preferred, they are not always available when or as long as needed. For this purpose, two- or more channel photometers were devised.

**2.3.1. Differential Photometry with single pixel and array detectors.** The development of pulse-counting photoelectric differential photometry is discussed at length in Milone, Sterken, & Young (2011). The Rapid Alternate Detection System (RADS) developed at the Rothney Astrophysical Observatory was inspired by the previous work of Walraven (1953) described to the present writer by his advisor, Adriaan Wesselink, who had seen the two-star photometer in action in South Africa. Like the most advanced version of Walraven's instrument, RADS operated in a 4-channel mode with two channels set on the variable and comparison star and two channels set on the sky nearby. The RADS function generator attached to the photometer head allowed setting of the duty cycle and positioning of each of the four channels, usually used for variable and comparison stars and empty sky areas near them. Although the system was devised and used to obtain data even in skies impaired by light cirrus,

when conditions permitted the precision in the differential photometry could exceed 1%.

Differential photometry is currently carried out with CCD and CMOS arrays which are generally favored over single-pixel detectors, and means of self-calibration have been devised to meet the challenge of calibrating many pixels. Howell (2011) discusses the history of array devices. With appropriate techniques, milli-magnitude precision is now obtainable. Software such as *IRAF* and *ESO-Midas* have been used for image processing and, with *DAOPHOT*, for the extraction of magnitudes and precise positions on the sky of each star in the field.

**2.3.2. Photometric calibration.** Typically PEP data of variable stars and one or more selected comparison stars are measured simultaneously, ideally, or alternately, to provide a differential light curve. Usually one or more comparison stars will be observed as a check on the constancy of the comparison star. The comparison and check stars must at some point be linked to a standard system by observation of standard stars in the same run. Landolt (1983) provided a list of standard stars that were spread around the equator for the benefit of astronomers in both northern and southern hemispheres. Procedures and the equations of condition for least squares determinations of extinction and transformation coefficients, can be obtained from various sources, the most classic being that of Hardie (1962). The subsequent modeling analysis of the data at some point must be converted into physical units, or at least solar values for the radii and masses, and astronomical units for distances within the binary system. Standardization is typically done by transforming local system magnitudes into standard system magnitudes; this requires observation of stars whose intrinsic magnitudes are known for the passbands of interest, such as  $m_{pg}$  and  $m_{pv}$ , the Johnson *UBV*, or the Strömgren *uvby* passbands, for example. Establishing those standards ultimately requires calibration. Calibration efforts for absolute photometry are critical for tying observational data into physical units. This effort similarly has evolved over time.

Photographic standard stars were established after  $\sim 1870$  when emulsions sensitive enough to record star images became available. A commission of the International Astronomical Union (IAU) was established in part to refine and coordinate efforts to do so. The North Polar Sequence of stars which could be widely observed from observatories in the northern hemisphere established such standards. Leavitt & Pickering (1917) present and discuss an early version of this important sequence for photographic and photo-visual magnitudes. This was subsequently replaced by other standards and in other areas of the sky for more modern passbands. Landolt (2011) and Sterken et al. (2011) discuss how procedures have changed over time and affected photometric precision and accuracy. Cohen (2011) discusses the history of photometric calibration efforts in the ultraviolet through the far infrared spectral regions, with relative and absolute methods, respectively, and Adelman (2011) does this for spectrophotometry. Considering that filter

photometry can be considered low-resolution spectroscopy, it may not be inappropriate to discuss in this section the calibration of other observables that can contribute to eclipsing binary analyses.

Stefanik, Latham, & Torres (1999) discuss the establishment of an absolute zero point for radial velocity measures for the standards established by the IAU Radial-Velocity Standard Stars group. The development of high resolution spectrographs with calibration lamps led to the detection of the relatively small orbital motions of stars due the presence of massive planets (Mayor & Queloz, 1995), as well as to the improvement of precision and accuracy of spectroscopic binaries. The development of CORAVEL to provide radial velocity data for stars observed with the Hipparcos mission instruments and the subsequent development of Elodie are important examples. One of the more recent developments for precise calibrations is the laser comb for superimposing precise wavelength lines along with the spectrum of interest on the same array detector.

The bounteous data from Gaia and other scanning space missions as well as ground-based survey instruments can be inspected with rapid machine methods for classification purposes and perhaps orbital information and indications of the presence of other stars in the system (see, for example, Kostov et al., 2025; Li et al., 2024; Mowlavi et al., 2023; Prša et al., 2022). As these preliminary results will require detailed follow-up studies involving ground-based instruments and telescopes, we now demonstrate with an example why follow-up observations may be needed to provide still higher accuracy and precision of the observable curves. In illustration, we now discuss the system HP Dra, an eclipsing binary discovered in data obtained by the Hipparcos mission, although the derived orbital period that was reported (6.6930<sup>d</sup>) was incorrect.

### 2.3.3. A Case Study of the Eclipsing Variable HP Draconis

In the fourth paper in a series to evaluate how well Gaia would perform in furnishing fundamental data from eclipsing binaries, Milone et al. (2005) presented their analysis of replicative data, the Hipparcos and Tycho photometry and Asiago radial velocities, for three eclipsing binaries. One of the systems selected was HP Dra, with an EA-type light curve. For this system, a more correct orbital period and an eccentricity were found. The masses were determined to a precision of 2% and the radius of star 1 to 3%; however the radius of star 2 was determined to a precision of only 10%. Each of the minima is  $\sim 0.02^p$  wide, and in a 10.76<sup>d</sup> period, the data acquisition in these phase segments was so sparse it degraded the determinations of the stellar radii and the temperature differences between the components. Thus, the Gaia proxy photometric data from the Hipparcos mission proved insufficient within the eclipses to provide as fully precise and accurate stellar radii as one could expect. Because the Gaia test case required data comparable only with that expected of the mission's instrumentation as specified at that time, all available data

were not used in the Milone et al. (2005) analysis. The situation was remedied in a follow-up study with the inclusion of 869 ground-based *BV* observations from Cracow Observatory and RV data from Haute-Provence Observatory (Kurpinska-Winiarska et al., 2000) in addition to the Asiago RV data used in the previous study. As noted in Milone et al. (2010), the photometry was carried out carefully and meticulously. We discuss the analyses in Section 3.2.2.

## 3. Light Curve Modeling and Analysis

### 3.1. Basic Modeling

By 1880, there were six known eclipsing variables and, according to Russell (1948), E. C. Pickering (1880) made the first precise theoretical calculation of the light variation from a stellar eclipse. As noted, Vogel's confirmation of the eclipse hypothesis defined the first discovery of a spectroscopic binary; his was also the first attempt to determine system elements, thus the first RV analysis of an eclipsing spectroscopic binary --- on the basis of six photographic plate observations. The classification of systems by light curve appearance will be shown to require improved models to describe them adequately. The early 20<sup>th</sup> century Russell binary star model assumed spherical stars for systems with Algol-like light curves [EA], and tri-axial ellipsoids for those that displayed  $\beta$  Lyrae [EB] or W UMa [EW] type light curves. Neither shape correctly matches the true shapes of stars in a close binary system, but were considered adequate for most of the observations of the time. The means to derive the elements of a system (the "inverse problem") and then to calculate the light curve from the derived elements (the "direct problem") were and are critical stages in light curve modeling. Subsequently, more comprehensive models became available to analyze and model systems which had been systematically excluded from the longer-period, far-apart systems traditionally studied for fundamental properties such as radii, masses, and luminosities.

**3.1.1. A Case Study Analysis of SZ Cam.** For one of the better determinations of fundamental data prior to modern light curve acquisition and analysis methods we consider the Wesselink (1941) analysis of the EB type light curve of SZ Cam, the acquisition of which was described in Section 2.2.

The data were averaged in groups and once the period was determined [ $P = 2.6984166(33)^d$ ], and the data phased, averages of  $\sim 10$  contiguous averaged points were taken to produce normal points, an essential step in an age of hand computation. In the analysis of the light and radial velocity curves that he obtained, Wesselink used a spherical star model, presenting a uniform disk, considered appropriate for stars of early spectral type at the time. The eclipses are partial only (although Wesselink found them nearly total, and the analyses were made of the light curves rectified of ellipticity and reflection

effects. He had rectified the light curve to remove the curvature outside of the minima, and applied corrections for limb-darkening and gravity brightening effects. Wesselink found the ellipticity, the tidal distortion expected from what he regarded as the Roche model hypothesis, to be 0.04 and 0.02 for the two components. He sought but found no evidence of the reflection effect in the cosine term of the light curve. These procedures were similar to those devised by Russell (1912a; 1912b) and Russell & Shapley (1912a; 1912b). The ratio of surface brightness ( $1.24 \pm 0.13$ ) was determined from depths of the minima of the rectified light curve, but the RV curve of only the more luminous component could be measured so that only the mass function was known for the secondary star. Given the period and semi-amplitude of the RV curve,  $v_1 \sin i = 100$  km/s,

$$F^{1/3} = (M_1 + M_2)^{1/3} \cdot [M_2 / (M_1 + M_2)] \sin i = v_1 \sin i \cdot P^{1/3} = 0.65 \pm 0.08, \quad (1)$$

which provides a method of determining  $M_2$  by iteration even if it is not small, if the inclination is known or is close to  $90^\circ$  and  $M_1$  is known accurately; see, for example, Milone & Wilson (2014, p. 746). That was not quite the case here. As only two of the four contact points can be seen in primary minimum (although the secondary provides suggestions of slope change near deep minimum in the  $m_{pg}$  light curve) neither the ratio of radii,  $k$ , nor the difference in brightness,  $\Delta m_{pg}$ , could be determined from the light curve alone. Therefore Wesselink computed least squares solutions for each of five values of  $k$  over the range 0.45 to 1, all of which fitted the primary minimum well enough, but the secondary minimum was best fit with his solution 5,  $k = R_2/R_1 = 0.45$ . Wesselink's solution yielded radii  $r_1 = 0.412a$  and  $r_2 = 0.185a$  where  $a$  is the semi-major axis. For this solution the inclination,  $i = 76.1^\circ$ , and the difference in the component magnitudes,  $\Delta m_{pg} = 2.00$ . With the best assumed values of the day for the distance, interstellar reddening and extinction, and other astrophysical information, Wesselink obtained radii of 7.5 and 3.3  $R_\odot$  and masses of 20.0 and 8.7  $M_\odot$  for stars 1 and 2, respectively, for a mass ratio  $q = 0.44$ , with the primary minimum a transit eclipse.

The photographic light curve was held to be unusually accurate by Kopal, who included the solution in his catalogue (Kopal & Shapley, 1956, pp. 168-169); in rediscussing it, Kopal obtained a mass ratio,  $q = 0.29$ , derived from the ellipticity. Wesselink's value for the fraction of the area of the eclipsed disk at mid-eclipse,  $\alpha = 0.96$  for his favored solution and his drawing of the system shows a near-total eclipse; Kopal considered it to be total. Kopal's reworking yielded radii of  $10.9 \pm 0.9$  and  $4.5 \pm 0.5 R_\odot$  and masses of  $21 \pm 4$  and  $6 \pm 1 M_\odot$ , respectively; these are the data entered in his catalogue.

Results from modern solutions are quite different although the overall system configuration is confirmed. Techniques such as rectification produce light curves that would be produced by uniform non-interacting stellar

spheres. Although capable of yielding reasonable parameters for some elements and parameters, a far better course is to model the tide- and reflection-related causes for the classical "oblateness" and "reflection" effects, as in WD models. See Milone, Wilson, & Hrivnak (1987) for a comparison of results from both types of methods in the analysis of the overcontact system RW Com. The SZ Cam system is in an open cluster (NGC 1502) and the close proximity of ADS 2984A and fainter stars makes photometry and spectroscopy challenging because of light contamination, but in this case these challenges were met. Nevertheless progress with instrumentation and modeling techniques have enabled even more exacting results to be obtained from this interesting system. A modern solution is discussed in section in Section 3.2.1.

### 3.2. The Development of More Rigorous Binary Star Models

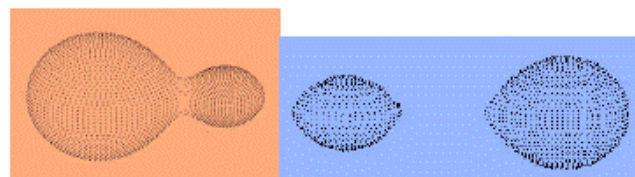
Recognizing the increasing availability of photoelectric light curves, and with the least squares element determination method of Piotrowski (1948), Kopal (1950), provided a more physically appropriate model for eclipsing binaries. In doing so, he and others built on the idea of gravitational equipotentials to describe the shapes of the component stars in close binary systems. This work ultimately stemmed from the treatment of the restricted three body problem by Lagrange (1772) and the subsequent fluid dynamic treatment of three body systems by Roche (1849, 1850). Kopal's (1959) equation (1-3) for the modified Roche potential of the binary may be written more generally as in Equation 2.

$$\Omega(r; q, d) = \frac{1}{r} + q \left[ \frac{1}{\sqrt{d^2 - 2\lambda dr + r^2}} - \frac{\lambda r}{d^2} \right] + \frac{1}{2} F^2 (q+1) r^2 (1 - \nu^2) \quad (2)$$

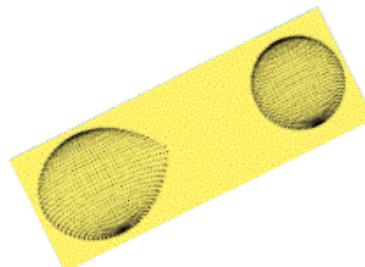
where  $r$  is the distance to the center of gravity of star 1,  $q$  is the mass ratio,  $M_2/M_1$ ,  $d$  is the separation of centers of the two stars (taken as unity by Kopal and Wilson & Devinney),  $\lambda$  and  $\nu$  are direction cosines, and  $F$  is the ratio of the angular rotational to the synchronous velocity, and is used to generalize the expression for non-zero eccentricity cases (Wilson, 1979). In the following decades, the basic model was turned into programming code. The potential expression has been divided by the factor  $GM_1$ , as per the expression used in publications by Wilson & Devinney (1971) and others who discuss his models. Among those who developed analysis programs to solve the inverse problem by deriving the elements of the systems and parameters relating to the component stars and produce synthetic light curves was Lucy (1968). Many other modelers were similarly developing models and methods as well, and their contributions are discussed in detail in Kalrath & Milone (2009). Except for the detached systems where neither star fills its inner lobe, the basic morphological configurations can be seen displayed in Figure 1: over-contact, semi-detached, and double-contact models.

### Modelling Stellar Surfaces as Lagrangian Equipotential Surfaces

#### Over-contact (over-filling lobe)



Double contact (thick disk)



Semi-detached (transparent disk)

Images courtesy, J. Kallrath

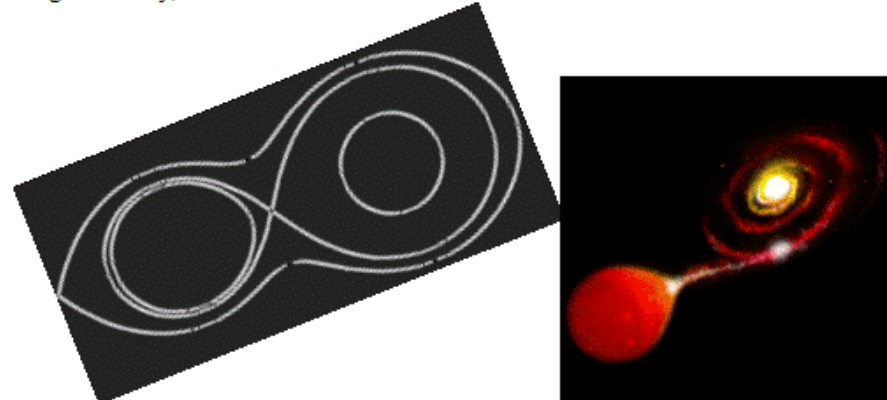


Figure 1: A pastiche of shapes of stellar surfaces as equipotential surfaces, defining the types of morphological models and informing their designations. From the top: left, an over-contact system (V728 Herculis, from Nelson et al., 1995) shown over-filling its inner Lagrangian surface; top right, a double contact binary with semi-transparent or opaque disk occupying one of the lobes and a lobe-filled donor star filling the other lobe; below them, on a tilt, a semi-detached system with the donor star filling its lobe but with a thin transparent disk around the other component star. That model is shown in a cross-sectional profile tilted to match the artful rendition of the system on the right. Individual figures, courtesy of Josef Kallrath.

Here we have focused on the models, methods, and programs of Wilson and his collaborators because the Wilson-Devinney program (hereafter, WD) is the most popular program and in more than fifty years of development it has continued to incorporate the best available physical models in order to determine optimum solutions for simultaneous analysis of multiple observable curves. Its many successive versions of accumulating features are described by Kallrath (2022) in detail. An online earlier WD program version called PHOEBE was developed by Prša (2018) who has now extended the

program to incorporate AI in order to evaluate and analyze large numbers of newly discovered Gaia and TESS eclipsing binaries as well as those from ground-based surveys.

The current code site and source for recent versions of the WD program are:

<https://faculty.fiu.edu/~vanhamme/binary-stars/>  
<ftp://ftp.astro.ufl.edu/pub/wilson/lcdc2015/>

It should be noted that Walter Van Hamme should be given credit for providing much of the updating over the last 30 years. The latest 2017 WD program version

includes 95 passbands (the 95<sup>th</sup> is for the TESS passband), the Kurucz and Phoenix model atmospheres for high and low temperature models, respectively, and all the other features of previous versions. The various modes available for use within WD constitute the WD models. The downloadable document *Binary Star Observables* is effectively the manual for the program and also contains details about the WD models. It contains sample input files for both the Differential Corrections (DC) and the Light Curve (LC) program routines. The *Observables* documents are updated for each new version and each contains a list of the changes applied since the previous version.

**3.2.1. SZ Camelopardalis Revisited.** Tamajo et al. (2012) used an enhanced 1998 WD version with Kurucz stellar models to analyze 40 high resolution RV data of both components, and 1517  $BVI_c$  CCD observations [with median total budget errors of 0.006, 0.001, and 0.007 for  $V$ , and  $B-V$  &  $V-I_c$  color indices, respectively, where  $I_c$  refers to Cousin's passband (bluer and narrower than Johnson's  $I$  passband)]. They obtained an equivalent determination of  $k = 0.75$ ; and  $q = 0.747 \pm 0.006$ ;  $\iota = 75.16^\circ$ ;  $R_1 = 8.91 \pm 0.05$ ,  $R_2 = 6.70 \pm 0.12 R_\odot$ ; and  $M_1 = 14.31 \pm 0.54$ , and  $M_2 = 10.69 \pm 0.38 M_\odot$ . With updated values of reddening and bolometric corrections, they determined the distance to be  $870 \pm 30$  pc, in agreement with the Gaia parallax value equivalent,  $849 (+69, -61)$  pc. From this we conclude that Wesselink's work, having an abundance of relatively precise observations and using powerful differential techniques, and uncovering the general nature of the system -- a transit eclipse at primary minimum -- nevertheless did not succeed in determining accurate values of the fundamental data partly because of incomplete data suites. In addition to being limited to one RV curve, and one photometric passband ( $m_{pg}$ ), and having to reply on a mass-luminosity relation for a value for  $M_1$ , the analysis could not include a major 3<sup>rd</sup> light contribution to the light curve --- that of a third component, discovered by Mayer et al. (1994; 2010) and confirmed through speckle interferometry by Mason et al. (1998). Tamajo et al. (2012) used a spectral disentangling technique to see the effects of the third star in the spectral line profiles of the  $H_\alpha$ ,  $H_\beta$ , and  $H_\gamma$ , which were also fitted with NLTE (non-thermal equilibrium) line profile models. The relative contributions of the three components agrees with the WD analysis that included the 3<sup>rd</sup> light parameter (26% in  $I_c$ ), to within 0.5%. This case study thus highlights the effects of light curve precision and instrumentation as well as innovative techniques and modeling tools on absolute parameter determinations. In Section 3.5 we describe other discoveries in this system.

Next we discuss analyses of data of the relatively wide EA type eclipsing variable HP Dra with data suite surrogates of that expected of the Gaia mission and subsequent analyses with a much enhanced and complete data suite.

**3.2.2. A Case Study Analysis of HP Draconis.** As noted in section 2.4, the reported analysis by Milone et al. (2005) was followed up by another, reported in Milone et al. (2010). Figure 2 illustrates the model fittings to the RV and Hipparchus data and illustrates why a follow up study was required. The latter study made use of additional 869 photoelectric BV observations and Asiago RVs augmented by CORAVEL and Elodie spectrometer data totaling 51 observations of each component. The Tycho data (with m.s.e. of single observation of  $\sigma_{BT} = 0.11$ ,  $\sigma_{VT} = 0.09$ ) were excluded from the analysis.

Even though later WD programs are even more efficient, have more features, and allow a wider range of parameters to be determined, it is instructive to relate selected capabilities of this version and how they were used for this particular analysis. The analysis made use of the 2007 WD version (Wilson & Devinney, 2007; Wilson, 2008), hereafter, WD07. WD makes use of a damped least-squares engine with damping coefficient,  $\lambda$  usually set to  $10^{-7}$ , but solutions were not significantly affected by other values. Runs were made in mode 2, appropriate for detached binaries. We adjusted simultaneously 13 non-curve dependent and two curve-dependent parameters for a total of 19 of parameters. The weighting of the data, the subsets that were run, and the modeling procedures are recounted in detail in Milone et al. (2010). Because WD07 was not self-iterating, thousands of individual runs across several series of models were carried out in order to explore the parameter space adequately. After each run, the main set and all ten subsets were run, and the parameters of the subset that promised the most improvement in the sums of squares of the curve fitting residuals (SSR) was adjusted; if the overall fitting error did not improve, then the next most promising was chosen, and so on until convergence was achieved in all ten subsets. The final errors were taken from the full 19 parameter set. At the end of one of the last series of runs, every parameter was altered, one by one, by positive and negative increments of  $1\sigma$ ;  $2\sigma$ ; and by much larger increments ( $10-100\sigma$ ). No significant changes were found in this series of checks. The fittings for this analysis can be seen in Figure 3.

The results: The radii,  $R_1 = 1.371 \pm 0.012$  and  $R_2 = 1.052 \pm 0.010 R_\odot$ , were determined to precisions of 0.88% and 0.95%; the masses,  $M_1 = 1.133 \pm 0.005$ ,  $M_2 = 1.094 \pm 0.007 M_\odot$ , to precisions of 0.44% and 0.64%, respectively. From these, the mean densities of the components are  $620 \pm 20$  and  $1325 \pm 47 \text{ kg/m}^3$ , and the gravitational accelerations are  $\log g_1 = 4.218 \pm 0.010$  and  $\log g_2 = 4.433 \pm 0.011$  (cg s) for stars 1 and 2, respectively.

No spectral analysis was carried out for this investigation, but the properties of the components are known well enough to place them on log plots of luminosity vs. temperature and radius vs. mass. M.K.W. examined the range of models of different ages and chemical composition on the Padova interactive Web site <http://stev.oapd.inaf.it/cgi-bin/cmd> based on Marigo et al. (2008). A grid of models was explored in steps of 0.05 in  $\log(\tau)$ , where  $\tau$  is the age in Gy, over the compositional range  $0.008 < Z < 0.030$ . A model with  $Z = 0.019$  and age 4.47 Gy (i.e., an isochrone of chemical composition and age similar to the sun) fit the components' properties best as revealed on two plots. See Figure 4 (Fig. 4 of Milone et al., 2010).

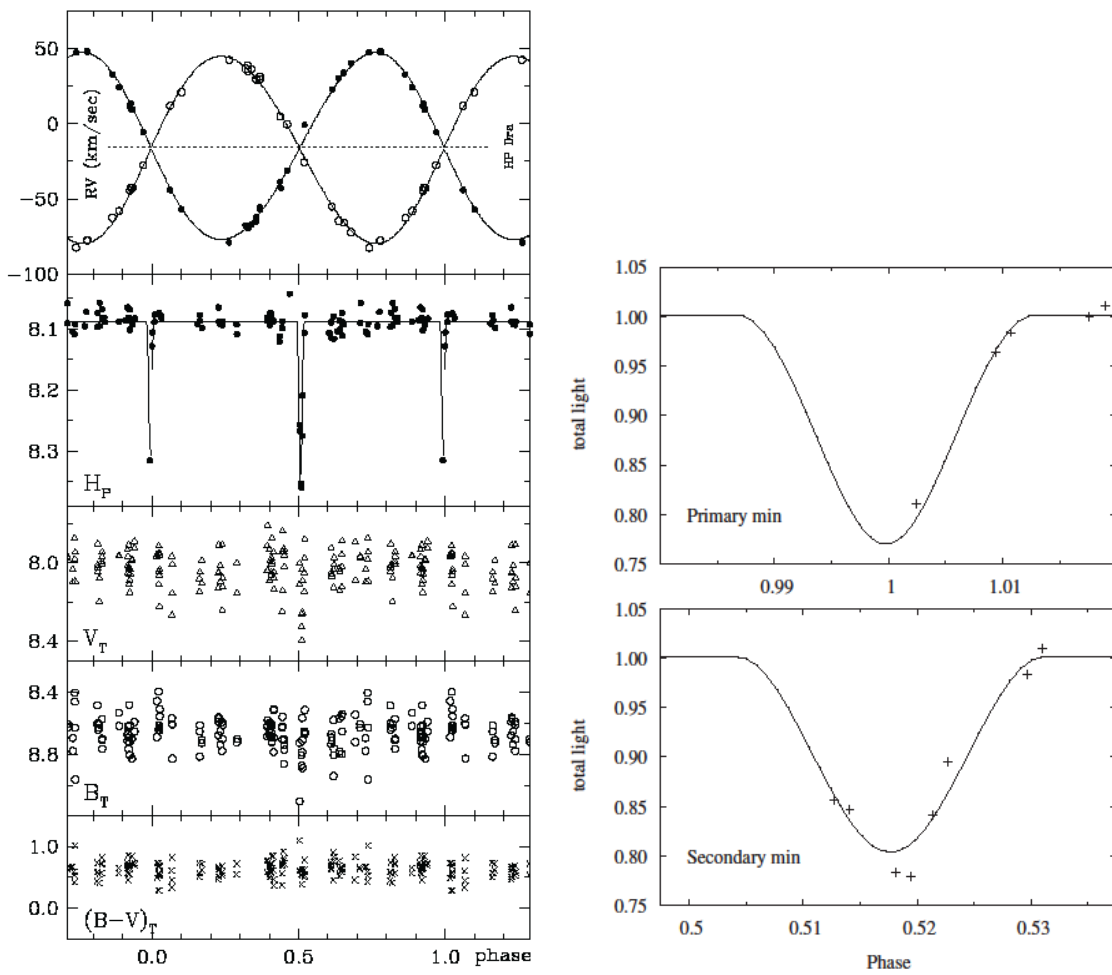


Figure 2: Phase-folded surrogate Gaia RV and light curves of HP Draconis from Milone et al. (2005). Left, from the top: Asiago RV curves, Hipparcos ( $H_P$ ), and Tycho light and color curves ( $V_T$ ,  $B_T$ , and  $(B-V)_T$ ). Right: blow-up of the  $H_P$  light curve primary and secondary minima and model curve. Note the sparse coverage in the minima of the  $H_P$  curve (and the large scatter in the Tycho curves) that when used alone limit the accuracy as well as the precision of the radii and luminosities.

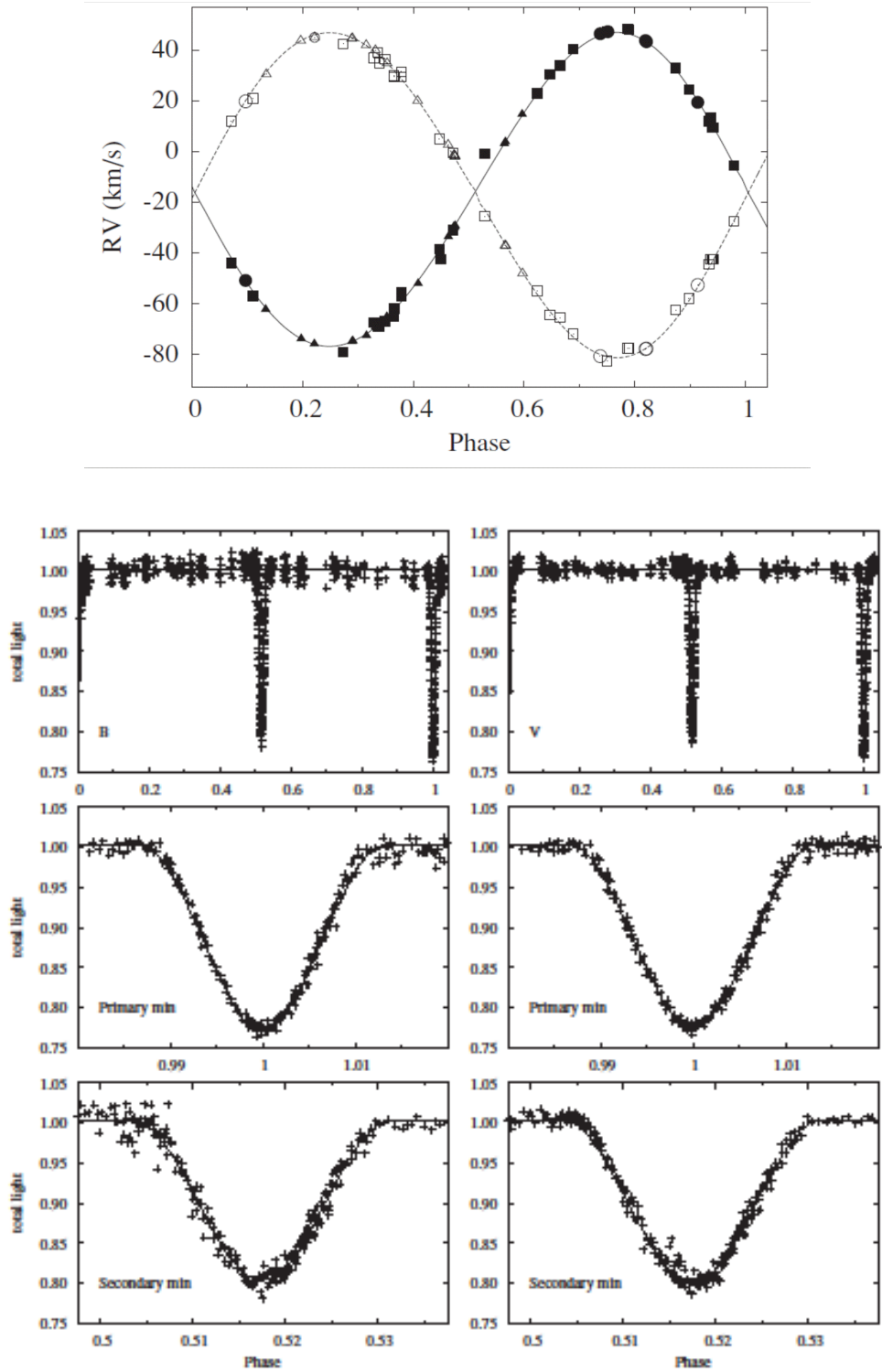
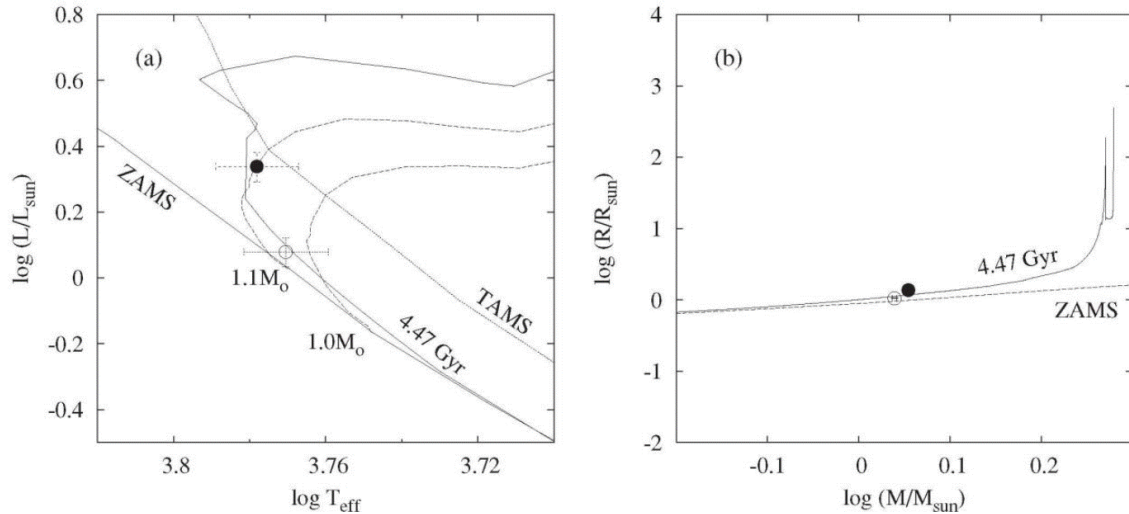


Figure 3: Phase-folded RV and light curves of HP Dra from Milone et al. (2010). Top: Asiago RV data represented by squares, CORAVEL data by triangles, and Elodie data by circles. Star 1 data have filled symbols; star 2 data have open symbols. Star 1 is the hotter and slightly more massive component. The discrepant point on the Star 1 RV curve just after secondary minimum received zero weight in the analysis. The curves of the final fitting are shown. Bottom:  $B$  (left) and  $V$  (right) full, primary minima, and secondary minima light curves of HP Dra and the fitted curves of the adopted model. Note the completeness of coverage. See Figure 2 for the  $H_P$  minima fittings.

### HP Draconis Primary and Secondary Components and a Padova Model



Source: Milone et al. (2010)

Figure 4: HP Dra components compared with the ZAMS on (a) a plot of  $\log(L/L_\odot)$  vs.  $\log(T_{\text{eff}})$  with evolutionary tracks for  $1.0$  and  $1.1 M_\odot$  stars, showing also the TAMS; and (b) a plot of  $\log(R/R_\odot)$  vs.  $\log(M/M_\odot)$ . The properties of the components seem to fit best (among the Padova family of models inspected) with the  $4.47$  Gyr isochrones. With this model, component 2 is seen to lie within  $\sim 1\sigma$  of the ZAMS. Component 1, with only  $3.4\%$  more mass than its companion, has evolved off the ZAMS but not as far as the TAMS. From Milone et al. (2010), Fig. 7.

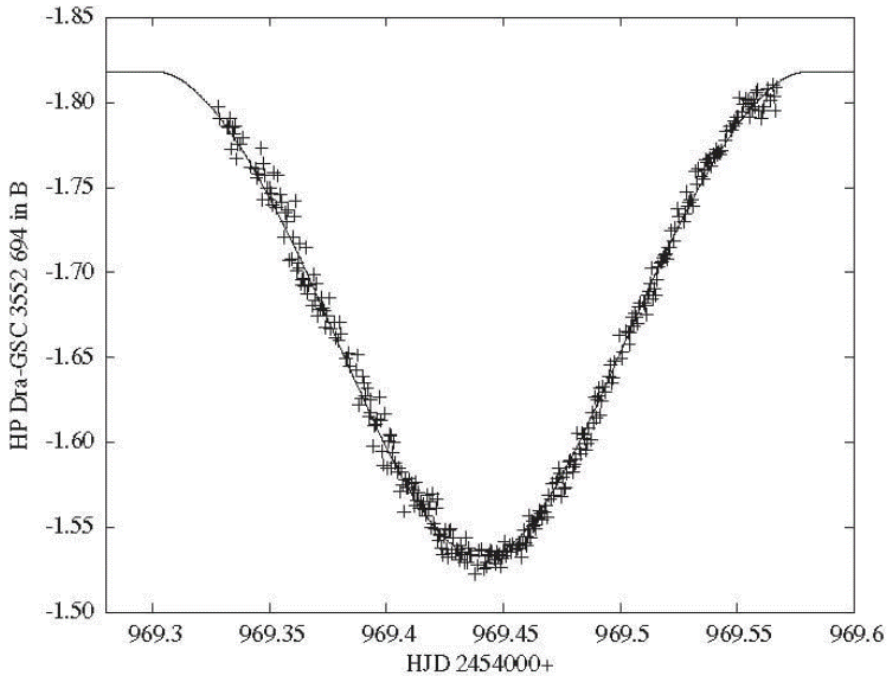
Finally, Cracow Observatory CCD observations at primary minimum, were obtained following the conclusion of the analyses and thus not used in them, are shown in Figure 5 along with the synthetic light curve from the model, computed for that interval of observation. Nevertheless it is curious that the secondary lies within  $1\sigma$  of the zero-age main sequence (ZAMS), whereas the primary that has less than  $4\%$  greater mass than the secondary is approaching the terminal age main sequence (ZAMS). Similarly odd is the condition that the primary has half the mean density of the secondary component. Perhaps there is more to be learned from the solar-analogue stars in this system. A spanking new study may help to provide some of it.

In August, 2025, Southworth (2025), hereafter S25, posted a preprint linked to the DEBCat website claiming a greater precision in the mass and even more in the radii determinations in this partial eclipse system. S25 made use of 14 sectors of TESS data, which are abundant, used the flux level in a narrow range on either side of the eclipses, and used a spherical model code, JKTEBOP, to analyze the minima. Of course use of a code that assumes stars to be spherical is usually safe enough if the stars are far enough apart and well within their inner Lagrangian surfaces. The WD program computed the sizes of the polar, inward-pointing, side, and back radii for the final model and demonstrates that they agreed with each other well within errors for each component, so an assumption of sphericity itself is not inappropriate in this case.

For components 1 and 2, S25 obtained for the masses:  $1.1354 \pm 0.0023$  and  $1.0984 \pm 0.0022 M_\odot$  and for the radii,  $1.2474 \pm 0.0046$  and  $1.1498 \pm 0.0049 R_\odot$ , respectively, noting that these are among the most precise absolute parameters for binary star components currently available.

S25 finds a much smaller third light:  $0.5\%$  vs.  $\sim 10\%$ , “and this changes the measured radii significantly.” S25 analyzed the light and radial velocity curves separately, unlike the Wilson-Devinney approach (where all data are solved simultaneously and where all weights, including curve weights, are carefully determined). The S25 approach provides the amplitudes of the radial velocity curves:  $K_1 = 61.971 \pm 0.056$  km/s,  $K_2 = 64.067 \pm 0.060$  km/s where the error bars are determined not by least-squares but by 1000 Monte Carlo simulations; this yields  $q = 0.9673$ . S25 “determined the distance to HP Dra using the BV magnitudes from Tycho, JHK<sub>S</sub> magnitudes from 2MASS and surface brightness correlations...” from another source. S25 “allowed an uncertainty of 0.02 mag, for the interstellar reddening” and states “Our most precise distance estimate is the K<sub>S</sub> band and is  $77.9 \pm 1.2$  pc,” which agrees with the Gaia DR3 parallax result of  $79.27 \pm 0.32$  pc. S25 found a solar composition model with  $3.5$  Gy age that adequately matches his results. Finally, S25 finds evidence for magnetic cycle activity in TESS light curve variations suggesting possible non-synchronous rotation by one of the components and by emission in-filling of Ca H & K line profile centers.

## HP Dra Analysis Model Verification



Source: Milone et al. (2010)

Figure 5: From Milone et al. (2010, Fig. 4), CCD differential  $B$  passband observations of HP Dra, obtained at Cracow Observatory on 2009 May 17 near phase zero, and plotted along with the light curve predicted from our adopted model. These data were not included in the analysis and thus represented an independent check on the results, including apsidal motion.

**3.2.3. Comparisons of HP Draconis Models and Results.** As the system is an important one to understand how stars like the sun evolve over time, it is important to understand any differences in determinations.

Milone et al. (2010), hereafter, MK-WO or *we*, found a distance also in agreement with the DR3 results, but with a stated error that reflects the uncertainties in the temperature scale ( $\pm 150$  K), in the absolute luminosities relative to the sun, in the interstellar extinction  $A_\lambda$ , and in the bolometric correction. S25 assumes the same  $T_1 = 6000$  effective temperature that *we* did, and that value is hardly without large uncertainty. The derived distance, 77 pc, agrees within errors with the distance previously derived from the *hip* and Asiago RV data alone,  $73 \pm 4$  pc. If *we* adopt,  $E_{B-V} = 0.00$ , as did S25, then the distance increases slightly, to  $80 \pm 3$  pc, in close agreement with the Gaia DR3 parallax result of  $79.27 \pm 0.32$  pc.

Although the S25 mass ratio is in agreement with the MK-WO adjusted parameter,  $q = 0.9658 \pm 0.0037$ , and the MK-WO and S25 masses similarly are in agreement, the radii are not; S25 finds the primary star to be 7% smaller and the secondary 5% larger than did *we*, a difference he ascribes to a larger amount of 3<sup>rd</sup> light. The claimed effect of third light on radii determination is unclear. It would be of interest to see the full details of how the S25 results and

uncertainties were obtained. Regarding the reality of 3<sup>rd</sup> light in this system, MK-WO comment: “As part of the exploration of the reality of the  $l_3$  quantities, runs were made with these values set to zero, and the results followed up through more than a dozen runs of successive changes. In each case, the preferred adjustment was to restore the value to the  $\sim 10\%$  level.” The source is yet to be determined, however. It would be of interest to see how S25 was able to improve on the radius determination and precision and to make a determination of third light in the system with the procedures described.

If improved precision arises from differences from averages in a large number of trials we note that such a determination of errors does not necessarily provide an accurate assessment of the true uncertainty. The question needs to be asked: are the individual run determinations truly independent? If not, one must be wary of claims of extraordinary precision. Additionally, systematic error, arising from sources outside the averaging process, must be considered.

To resolve discrepancies and explore this partially eclipsing system further, a number of systematic adjustment of the potentials to produce a grid of sizes for each component as suggested by D. Terrell (2025, private correspondence), and use of features of later WD versions

(>2013) to analyze the now further enhanced data suite, with the eclipses timings, the Ca line profiles, and, as S25 suggests, further spectral analysis to determine more precisely the chemical composition of the system. More recently adjustable parameters are  $\log d$  (via the direct distance estimation), interstellar extinction,  $A_\lambda$ , as well as star spot property and aging parameters, and third body dynamical parameters; with updated solar values and other constants, analysis then may yield tighter fittings and more accurate results, and provide information about the dynamics of any other components in the system. Given strong confidence in the Gaia distance, the IDE (inverse distance estimation) can be used to strengthen the determinations of other parameters. The differences between the Asiago assessment of approximately solar composition, the previous lower metallicity estimates based on Strömgren system photometry, and the suggestion of a slight improvement in the residuals with a higher metallicity, all point to a need for further spectral analysis. Given the question of third light and the apparently relevant  $d\omega/dt$  and  $dP/dt$  parameters despite large internal errors, in addition to adjusting WD third body parameters, speckle interferometry, as we note below, could be revealing.

It is clear that the results from analysis of the initial Gaia-simulation using Hipparcos +Tycho +Asiago proxy data are superseded by those from larger, improved data sets. Later results are among the most precise determinations of fundamental stellar data that have been made. With the discoveries of S25, even further characterization appears possible.

And this leads us back to further opportunities for high precision photometry and to a broader range of spectral coverage, to uncover the spectral distribution of any third light sources.

### 3.3. Disk Models and Double Contact Systems

Beginning in 1979, Wilson turned his attention to proposed disks surrounding an unseen companion in systems such as  $\beta$  Lyrae. The basic idea was to approximate the self-gravitation of a circumstellar disk by that of a massive but infinitesimally thin wire-like ring concentric with the star at the center of the disk, analogous to conceiving of the stars in the Roche model as represented by central massive points. This led to the expansion of Equation 2 to include the gravitational potentials of stars 1 and 2, the centrifugal potential, and the gravitational potential of the massive wire ring lying in the orbital plane, resulting in the total modified potential for such a binary star system (Wilson 1979, 1981, Eqn. 1) in Equation 3.

$$\Omega = \frac{1}{r} + q \left[ (D^2 + r^2 - 2r\lambda D)^{-1/2} - \frac{r\lambda}{D^2} \right] + \frac{(1+q+q')F^2 u_1^{-2}}{2(n+1)} \left[ \left( \frac{u}{u_1} \right)^{2(n+1)} + n \right] + \frac{q'}{\pi(2R)^{1/2}} \int_0^\pi \frac{d\phi}{[(R^2 + r^2)/2R - u \cos \phi]^{1/2}}. \quad (3)$$

where the quantities  $r$  and  $\phi$  are polar coordinates with  $r$  measured from the center of star 1,  $D$  is the instantaneous

separation of star centers,  $R$  is the radius of the wire ring in the disk's equatorial plane,  $\lambda$  is the direction cosine of the line of centers,  $n$  is a constant so that the angular velocity is proportional to  $u^n$  where  $u$  is the distance of a point from the rotation axis of star 1, and  $u_1$  is the null point of effective gravity for the (uniformly) rotating primary star. It defines the outer limit of the disk; another null point defines the inner limit. Given  $n$ ,  $F$ , and  $u_1$  the angular rotation speed, the centrifugal potential and the centrifugal force are everywhere determined.

Wilson (2018, Fig. 12) applied the accretion-decretion (A-D) self-gravitating disk model to a differential V light curve of  $\beta$  Lyrae, the prototypic EB eclipsing variable, with a hot less-luminous supergiant (B8 Ib) component, and a component long considered to be completely enshrouded within a disk.  $\beta$  Lyrae was among the five eclipsing binaries that Plavec & Koch (1978) reported to have strong far ultraviolet emission lines and continua and were later (Plavec, 1980) referred to as W Serpentis stars, after the system with the strongest emission and a clear view of the disk component that is far more luminous than the donor (unlike the case with the brightest member of the group,  $\beta$  Lyrae). They noted that

"The high level of ionization indicated by strong emission lines of Si IV, C IV, and N V is remarkable. It is not yet clear from which region or regions of the systems these emissions come. One possibility is a high temperature, low density plasma surrounding the hotter component. It should be noted that the hot component may well be the spectrographically invisible one if it is surrounded by an optically thick disk of gas."

The disk in the  $\beta$  Lyrae system has the lower surface brightness, enshrouding an unseen, star.  $\beta$  Lyrae is an SB1 system; only the donor star's spectral lines have been observed. Wilson's (2018) preliminary trial-and-error fitting (Fig. 12) is reproduced and annotated in Figure 6. The data are from the Villanova APT instrument; original observations are in Abt (1995). In the deeper eclipse, the disk is eclipsing the B8 Ib lobe-filling donor star; other eclipse is of the disk by the donor. The light variation between eclipses is attributed to tides in the disk and donor. In Wilson's basic disk model there is natural closure of level surfaces without arbitrary disk truncation. Tidal stretching of the disk by the donor star enhances overall tidal brightness variation. The light curve has been relatively stable over centuries, so the high accretion rate, characteristic of a binary in the rapid stage of mass transfer, requires the accreted material to be either absorbed by the non-compact star at the disk center or, as Wilson (2018) suggests, decreted back into the disk. In either case it is a DbC and a strong candidate for an A-D disk system. In some Algol systems, the emission line features may be seen only in the deep minimum implying that the disk is consequently thin and not massive enough to be self-gravitating. In such systems the recipient component readily absorbs the accreted material and can drain the disk on short time scales.

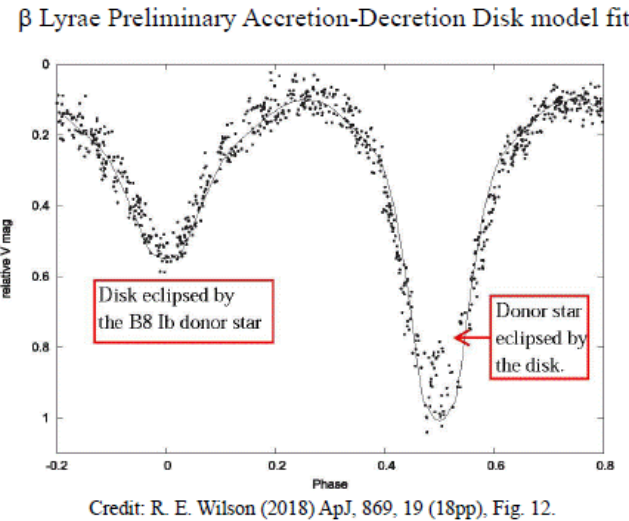


Figure 6: From Wilson (2018, Fig. 12), a preliminary trial-and-error fitting of the A-D disk model to a differential V light curve of  $\beta$  Lyrae. The data are from the Villanova APT instrument; original observations are in Abt (1995). In the deeper eclipse, the disk is eclipsing the B8 Ib lobe-filling donor star; other eclipse is of the disk by the donor, so the B8 Ib component has a higher surface brightness than the disk.

Whereas the  $\beta$  Lyrae light curve is relatively stable, that of CI Aquilae is not; it is a recurrent nova. Figure 7 (from Fig. 6 of Wilson, 2018) shows a fitting for the eclipsing cataclysmic variable (CV), CI Aql, in quiescent state after its eruption in 2000. The photometry data are from Schaefer (2011, 2014) and Wilson & Honeycutt (2014) and the RVs are from Sahman et al. (2013), who made ingenious use of Doppler tomography to secure velocities from the line profile wings of the disk as proxy values for those of the white dwarf. Wilson (2018) provides evidence that if they are massive enough A-D disks around the nova may survive moderate outbursts. That a similar light curve is seen before and after the last outburst of CI Aql proves that its disk has done so. In the present instance, the model allows the disk to be semi-transparent so that when it eclipses the donor star, some light is able to diffuse through the disk and the “oblateness effect” in the maxima is due not so much to the lobe-filling donor, but mainly due to the lobe-filling tidally distorted disk. In this case the hidden star is a white dwarf, spun up by the angular momentum of the disk material to the point of decreeing it back into the disk. Consequently in this Dbc case, the disk is massively self-gravitating and undoubtedly an A-D disk system. Wilson & Hunnicutt (2014) treat the dynamics of the stream and disk.

The modeling of disks in double contact (DbC) systems uncovers some interesting and even surprising results. Aspects of the equipotential disk include its semi-transparency to allow both attenuation and re-emission and the irradiance of the companion star, and the reflection functions defined in Wilson (1990) provide the efficiency to allow multiple reflections. An inner null point defines the inner edge of the disk; both null points are computed at each iteration. As a consequence, there is no arbitrariness in defining the confines of the disk; they are determinable in the model. In their recent work, Wilson & Van Hamme (2025) emphasize a number of details about the cases of CI Aquilae and U Scorpii where the disks contain 3% and 6% of the white dwarf mass, respectively:

1. The white dwarf's rotation is coupled analytically to disk properties such as size and shape that affect the photometric variation via the A-D condition;
2. The parameter  $F$  (the ratio of the white dwarf angular rotation to the orbital angular rate) is a parameter that can be adjusted and so is determinable;
3. The orbital rate is known from the orbital period and size, hence the rotation rate and Period;
4. The outer disk edge parameter,  $x_{\text{outer}}$  is found to be close to  $x_{\text{null}}$  where the effective gravity is zero, within errors. This constitutes a check on the model.

It is possible and may even be likely that many if not most post-novae are double contact binaries. The Dbc model should lead to more precise determinations of the properties of these objects. More observations are needed of CVs and novae in quiescent states. Two eclipses are needed for modeling and because the disks are typically hotter than the donor stars, IR photometry will be useful.

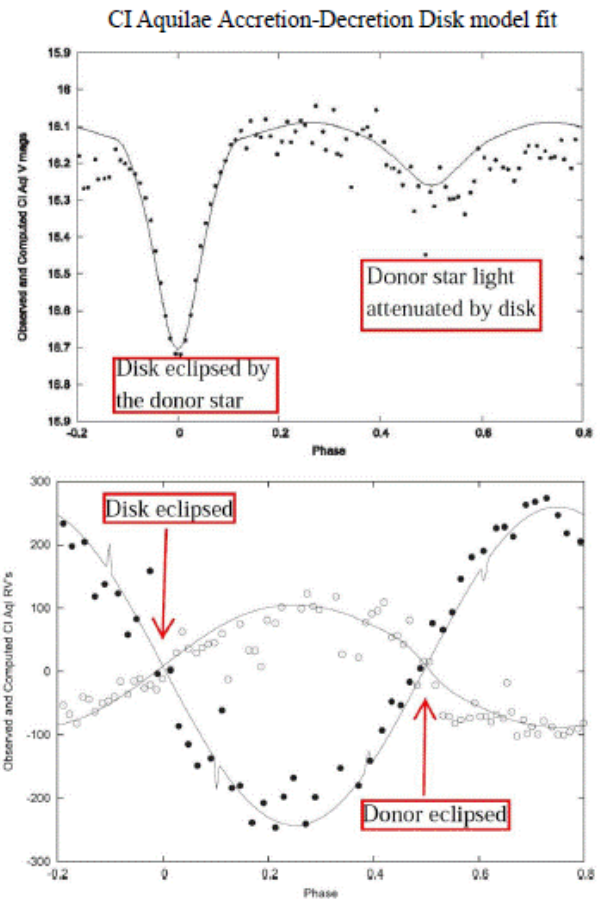


Figure 7: From Wilson (2018, Fig. 6), the V passband binned light curve (top) and radial velocity curves (bottom) of the recurrent nova CI Aql in quiescent stage together with the preliminary fitting to them of an A-D disk model. The light curve data are from Schaefer (2011, 2014) and Honeycutt & Wilson (2014), the RV data from Sahman et al. (2013). The open circles are donor RVs and the closed circles are disk RVs; the latter are based on emission line wings, considered proxies for the white dwarf itself. The deeper eclipse at phase 0 is of the disk by the donor star. The shallower, broader eclipse is of the donor star by the semi-transparent disk.

### 3.4. Ancillary Software

Over the decades that this astronomer has been working much ancillary software has appeared which have proven very useful in light curve analysis. These include algorithms to seek out the deepest minimum in parameter space with efficiency, such as Simplex, and robustness, such as Simulated Annealing (SA). Both are fully referenced and discussed in Kallrath & Milone (2009). A version of SA was implemented by Kallrath within a package coupled directly to WD07 (described above). Tests of this SA version, discussed in Milone & Kallrath (2008) was used in the analyses of newly discovered eclipsing binaries in a field of the RAO's Baker-Nunn patrol camera by Williams & Milone (2013). Currently D. Terrell is using the algorithm in addition to the 2013 WD version in his study of V372 Draconis.

Doppler tomography as used in *Shellspec* (Budaj & Richards, 2004) is a very promising way to check the dynamical layout of close binary systems; Janos Budaj (2025, private communication) relates that the latest public release is Shellspec49 but that such advanced features as dust reddening and extinction, definition and treatment of shadows by opaque objects, and the introduction of ellipsoidal disk like structures is being incorporated into the program. See Budaj, Maliuk, & Hubeny (2022) for its use in modeling an exotic white dwarf system.

Spectrophotometry has not been mentioned thus far, but if it can be done to avoid stray light issues, it can produce a boon to ground-based acquisition of a large number of light curves across the spectrum simultaneously. Such as instrument in fact has been designed and built for absolute calibration purposes. Adelman (2011) discusses the history of spectrophotometers and scanners and a specially made optical telescope telescope to avoid light loss and scattering.

Polarization measurements, although challenging to make, are also worth pursuing, given the importance of magnetic fields in systems with compact components. Bastien (2011) discusses the history of polarimetry and its usefulness in discerning electron scattering envelopes in binary components and even in the determination of orbital elements. It may be especially useful in studying DbC systems. One important instrument for this purpose is *ESPaDOnS*, a bench-mounted high resolution echelle spectrograph/spectropolarimeter, available at the Canada France Hawaii Telescope (CFHT). Bailey et al. (2023) report on recent high-precision polarimetry and new results with *PICsarr* (Polarimeter using Imaging CMOS Sensor And Rotating Retarder).

Finally, speckle interferometry can confirm the presence of additional objects within a binary star system, as we note below.

### 3.5. The Study of Hierarchical Systems

With improved models, attention returns to improving the precision and accuracy of the observables. One area that is emerging is the extent to which binary stars are parts of greater systems, hierarchies. This impacts the analyses of eclipsing systems in such configurations.

Improved light curve coverage is providing accumulated evidence of hierarchical stellar systems with binaries and a third component having the simplest such configuration. Pribulla & Rucinski (2006) found that a significant number of W UMa systems had wider companions. Similarly, Nelson et al. (2023) in searching for solid evidence for mass exchange in W UMa systems, found many examples of other components in time-of-minimum analyses. Although sixty systems were investigated, in the end only seventeen presented sufficiently strong evidence for mass exchange. This was due, in large part, to insufficient coverage of the orbits of additional companions to the eclipsing binary systems to satisfy the light time effect (LiTE) analyses of the period variation.

Hierarchical components have been studied spectroscopically and astrometrically by Tokovinen (2025), who notes that the Gaia mission detection of such systems is quite incomplete. Therefore, like systems discovered through minimum timing in eclipsing systems, extensive ground-based follow-up observations are needed to provide the full picture. Starting with visual binaries, he probes the inner components. Some of his studies are of historical interest as well; in one case, a visual binary separated by 3 arc-sec when discovered by John Herschel in 1837 (HJ 4310, HIP 49442), is found to be a multiple star system. The brighter component, A, has a companion only 0.18 arc-sec apart as revealed by Speckle interferometry: components Aa and Ab. But the spectrum of A reveals three set of lines; component Ab is itself a binary system (Ab1, Ab2) separated by 0.0098 arc-sec, making them part of a quadruple system of 3+1 hierarchy. The masses of the A components need to be refined, requiring more observations.

According to Tamajo et al. (2012), SZ Cam, in addition to being the northern component of the visual binary ADS 2984, has another component, discovered through speckle interferometry, and it is a single-lined spectroscopic binary system (SB1). One of the four stars is a  $\beta$  Cephei pulsating variable. More recently, the southern component of the visual binary with SZ Cam, ADS 2984A, has been found to be an SB1 system (Gorda, 2016). If all these reports are correct, SZ Cam is in a system of six stars, all of which would be members of the young open cluster NGC 1502.

From an entirely different area of study, evidence for a systemic acceleration during a black hole merger led S.-C Yang et al. (2025) to propose that the merger occurred in the vicinity of another, possibly supermassive, black hole. Disks around SMBHs have been suggested as a site where smaller black holes could merge, creating the unexpectedly large masses found for increasing numbers of them from LIGO event studies.

## 4. The Promise of Precise Infrared Photometry for Future Light Curve Analyses

Almost all the photometry discussed above was done in the visible part of the spectrum, but the Earth's atmosphere also has windows in the infrared part of the

spectrum ( $\geq 1\mu\text{m}$ ; hereafter IR, but not to be confused with Johnson's "red"  $R$ , and "Infrared"  $I$ , passbands). Analyses now are able to make use of the milli-magnitude-precision achievable from ground-based optical photometry. Up to the present, that has not yet been achieved to the same extent in the infrared.

In systems with greatly contrasting components, the IR will help to define the secondary minima so that temperature differences, modified Kopalian potentials, limb-darkening, albedos, and gravity-darkening coefficients may be determinable with unprecedented precision. The smaller contrast of cool spot temperatures in the IR, combined with other passband data, will permit better separation from the overall morphology to produce improved spot temperature, longitude, size, and, for central eclipses, perhaps also latitude.

Algol's B and V light curves defined its EA light curve character but its infrared light curve resembles an EB type. A posting at the American Association of Variable Star Observers (AAVSO) website notes the importance of continually observing 12.9<sup>d</sup>-period  $\beta$  Lyrae in the infrared as that system evolves (Terrell, 2025). A DBC system in which the disk is radiatively cooler than the donor is a good target for IR work. Wilson (2025) notes that a  $B$  light curve does not show a secondary eclipse in the recurrent nova U Sco whereas an  $I$  light curve does. This system may be a good target for photometry in the even redder passbands discussed below. The system DS And is a 1-day period, double-lined eclipsing binary in an open cluster (NGC 752), and both recent major analyses of the system (Milone et al., 2019; Sandquist et al., 2022) although arriving at different absolute parameters (at least some of which may be due to the re-reduction of RV data), find anomalies in one or both components. In such a case, additional types of data and perhaps new stellar models need to be considered and explored.

Now we describe the status of infrared passbands, the challenges in carrying out photometry with them, and how those challenges can be met.

IR Photometry can produce high photometric precision in principle because:

- 1) there is little atmospheric Rayleigh scattering ( $\propto \lambda^{-4}$ ) in these wavelengths; and
- 2) there are now passbands that minimize the parts of the windows with absorption bands of water vapor and other atmospheric molecules.

The Earth's atmosphere is not as transparent to radiation beyond 1  $\mu\text{m}$  as is visible light, because of molecular absorption bands, mainly from water vapor, which is variable on all time scales. There are however spectral regions where the absorption is minimal, referred to as atmospheric windows. As part of a multi-color, wide-band set of passbands that included *UBVRI*, Harold Johnson (1964; 1966) defined for the region between 1 and 4  $\mu\text{m}$  the passbands  $JKL$  ( $H$ , between  $J$  and  $K$ , was added later), and for the  $>4$  to 22  $\mu\text{m}$  region  $M$  and  $N$  ( $Q$  was added later). With relatively insensitive detectors and limited options, the filters selected to sample these regions were so broad they overlapped atmospheric windows, so

the passbands are partly defined by the varying water vapor absorption. Several attempts were made by astronomers to narrow the passbands somewhat to improve the resulting problem with precision and repeatability of the IR photometry at their sites, resulting in many versions of the Johnson passbands, and yet all bearing the same Johnson designations. The problem with contemporary IR astronomy, how astronomers dealt with it, and how it could be improved, was discussed at length at a joint meeting of IAU commissions 9 and 25, at the IAU General Assembly in Baltimore in 1988 (Milone, 1989). The problem was identified and resulted in the creation of a Working Group to fix it. The work was described and preliminary results were reported in Young et al. (1992). The history is summarized in Milone & Young (2011).

Young et al. (1994) noted that the  $J$  passband included a strong water-vapor band at 1.14  $\mu\text{m}$  and proposed replacing that  $J$  passband with two passbands on either side of the water vapor band: a new passband we called  $z$ , after the Kodak Z sensitization class which was useful for this spectral region, and an improved  $J$  on the long-ward side of the absorption band. Later we referred to the improved  $J$  passband as " $iJ$ " and the  $z$  passband " $iZ$ " for consistency. The 1  $\mu\text{m}$  window we refer to as the  $Z$  window, and that beyond it as the  $J$  window. Similarly, we referred to the other windows with the designations formerly accorded to the Johnson passbands in which each of them was most centered and we placed a lower case letter  $i$  in front to designate the new passbands, hence  $iH$ ,  $iK$ , etc. The recommended change in usage for the  $ZJHKLMNQ$  designations was formally approved by the International Astronomical Union: IAU Resolution B1, *on guidelines for the designations and specifications of optical and infrared astronomical photometric passbands*, that was put forward on behalf of Commission 25 and its Infrared Working Group (IRWG) and passed at the 2012 Beijing General Assembly. The resolution states in part that "the designations  $ZJHKLMNQ$  should be used henceforth to refer exclusively to the terrestrial atmospheric windows in the near and intermediate infrared (see Young et al. A&AS, 105, 259-279; Milone & Young (2005), PASP, 117, 485-502)."

As a consequence, while primes and subscripts on the old passband names have proliferated, amid a continuing use of the old names by some astronomers, newer passbands have rarely been optimized for use at all elevations and atmospheric models. Even those designated as "short" passbands, such as  $K_s$ , though trimmed to be less affected by water vapor absorption at high-elevation observatories such as Mauna Kea (4.2 km), fail to perform as well at lower sites in varying atmospheric conditions. The IRWG-designed passbands central wavelength placement and bandwidth were optimized to avoid the obscuration within the windows by minimizing the diminution of each of two Kurucz model stellar flux bundles traversing the atmosphere. The full methodology is presented in Young et al. (1994), and the realization of the near-IR suite of the recommended

passbands, through testing *iZ*, *iJ*, *iH*, and *iK* filters manufactured within specifications by Custom Scientific of Tucson, Arizona, is described in Milone & Young (2005, 2007), among other references. It is necessary to add, however, that photometry with unoptimized passbands carried out at a high and dry site under photometric conditions can be precise and accurate, and astrophysical relations among color indices valid. Wing (2011) notes that because basic information content of three-color photometry in the JHK windows is governed by the effects of stellar H- opacity the information content is not expected to change with the use of the IRWG passbands in these windows.

The upper portion of Figure 8 demonstrates the obscuration in atmospheric Z and J windows mainly due to molecular absorption by water vapor. The atmospheric transmission was computed with the MODTRAN program (Berk et al., 1989) for a standard atmosphere and a site at 1 km elevation above sea level. Superimposed are the passband profiles for *iJ* and *iZ* and their Custom Scientific equivalent filters, *cyJ* and *ciz*; *rJ*, is a Johnson *J*-like passband. The lower plots show simulated Bouguer extinction curves for the *J*, *iJ* and *iZ* passbands, all with the same stellar flux sources for a mid-latitude summer atmosphere at elevation of 1.3 km, the elevation of the RAO. Note the strong Forbes effect, the curvature of the extinction curve upward between 1 and 0 airmass for the *J* passband due to molecular absorption high up in the atmosphere. Actual extinction curves for Vega with *cyJ* and *ciz* passbands, on a particular night are shown in the lower right. In these passbands the extinction coefficients are low and the extrapolations to zero airmass give sufficiently close approximate to the outside the atmosphere magnitudes that differential photometry with well-chosen comparison stars, promises accurate and precise results.

A drawback in carrying out long-wavelength photometry has been that specialized telescopes and equipment have been needed. In the thermal IR, beyond  $\sim 3\mu\text{m}$ , liquid nitrogen or liquid helium cryogens are needed to reduce noise, and for single pixel detectors the sky background must be measured alongside the target stars, by rapidly chopping (oscillating) the telescope's secondary mirror, nodding the telescope to sample the opposite sky area, and using a lock-in amplifier and integrator to remove the sky signal and measure the flux. Consequently, IR work has usually been carried out only at observing sites at high elevations to minimize water vapor absorption and justify the expense of the operation. The latter constraint has been eased. The former constraint now also has a remedy.

Figure 9 shows the simulated spectral transmission of a mid-latitude, summer atmosphere at a site elevation of 300 m. Superimposed on this are the profiles for near-IR

IRWG passbands, *iZ*, *iJ*, *iH*, and *iK*. Note that they are not defined by the opaque edges of the windows, whereas wider passbands would be. It can be appreciated therefore that under such conditions the IRWG set cannot be called "narrow-band" in any real sense, and once signal to noise ratios, efficiency, and quality of the photometry is considered, they can be called "improved."

Recent work by Mishra & Kamath (2022) has confirmed this work and demonstrated the feasibility of using the three shortest IRWG passbands at observatories at both high and low elevations to obtain infrared light curves of improved precision and accuracy. Planning is underway at one site to realize that, in order to study population II pulsating stars among other targets (Mishra et al., 2024). Indeed in pulsating stars the IR is more sensitive to radius variation. Mishra & Kamath (2022) note the suitability and commercial availability of InGaAs single-pixel and array detectors and of additional filters that approximate the specifications for the *iZ*, *iJ*, and *iH* profiles. They provide a table of integration times to achieve  $\text{S/N} = 100$  per observation of stars with *J/H* magnitudes between 7.5 and 12.5 with four different detectors on a 1-m telescope, with dark current and read noise specified for the array detectors and NEP for the single-pixel devices.

The Mishra and Klamath work involves the non-thermal IR, but the full suite of IRWG passband recommendation extends much further into the IR. Just as the RAO, located at 1.3 km elevation above sea level, found it worthwhile to invest in thermal IR instrumentation in the 1980s into the early part of the current century, other observatories may find it equally worthwhile to do so. Figure 10 demonstrates the case for observing in the *N* ( $10\mu\text{m}$ ) window by comparing the obscuration and simulated extinction curves for old (*N*) and newer (*coN*) versions of Johnson's passbands in this window, and two IRWG passbands optimized for the main part and a smaller part of the *N* window, *iN* and *in*, designated here by *yN* and *yn*, temporary designations in Young et al. (1994). The lower four plots are simulated extinction curves for the *N* and *yN* passbands. Plots on the left, are computed for a tropical atmosphere and a site of 4.2 km; plots on the right, are computed for a mid-latitude, summer atmosphere at  $\sim 1$  km altitude. Note the decreased Forbes effect with the *yN* passband even for both elevations.

Future IR discoveries made with the James Webb (JWST) and Nancy Roman Space Telescopes likely will require follow-up data from ground-based observatories. Experience teaches that observing proposals seeking to monitor individual variable stars are rarely allocated observing time at premier observatories. Observatories at lower elevation sites able to invest in IR infrastructure and instrumentation can provide the opportunities to fill that need.

## Z and J atmospheric windows, J, iJ &amp; iZ Passband profiles and extinction curves

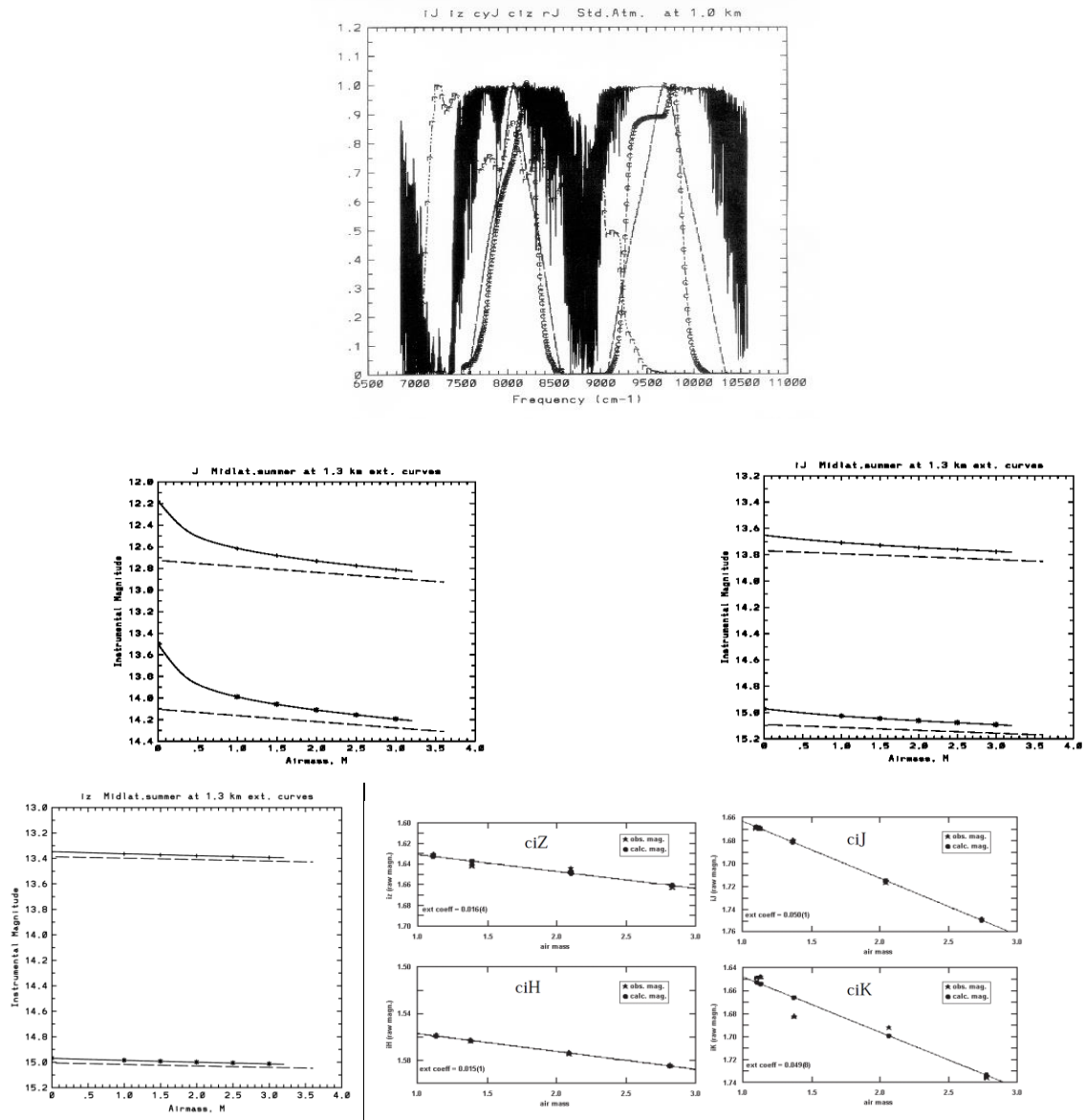


Figure 8: The top plot shows the spectral transmission between 0.9 and 1.5  $\mu\text{m}$  of a standard atmosphere computed with the MODTRAN program (Berk et al., 1989). It is plotted in wavenumber units of frequency. A value divided into 10,000 gives the wavelength in  $\mu\text{m}$ . The Z ( $\sim 1\mu\text{m}$ ) window is thus to the right and the J ( $\sim 1.25\mu\text{m}$ ) window to the left. Also plotted are the  $i_Z = iZ$ ,  $iJ$  and Custom Scientific filter profiles  $ciZ$ ,  $ciJ$ , and an older Johnson  $J$  passband previously used at the RAO,  $rJ$ , designated by first letter in the plots. Three of the lower plots, show simulated Bouguer extinction curves for  $J$ ,  $iJ$  and  $iZ$ , all with the same stellar flux sources for a mid-latitude summer atmosphere at elevation of 1.3 km, the elevation of the RAO. Note the strong Forbes effect, the curvature of the extinction curve upward between 1 and 0 airmass, for  $J$ . Actual extinction curves for Vega with the Custom Scientific filters approximating  $iZ$  and  $iJ$  on top and  $iH$  and  $iK$  (prefixed with "c") on the bottom, on Sept. 26, 2000 at the RAO, are shown in the bottomright set of four plots.

### Near-infrared Atmospheric Windows and IRWG Passband Profiles

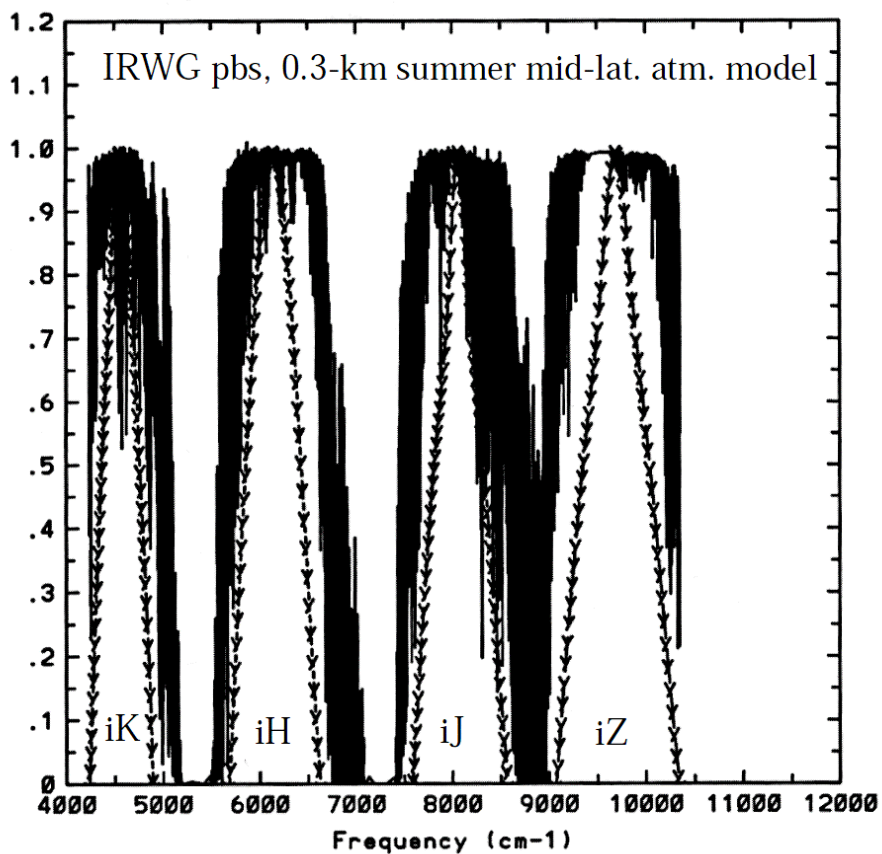


Figure 9: The simulated spectral transmission of a mid-latitude, summer atmosphere at a site elevation of 300 m, computed with MODTRAN software. Superimposed on this are the profiles for the near-infrared IRWG passbands  $iZ$ ,  $iJ$ ,  $iH$ , and  $iK$ . Note that the passbands fit comfortably into the atmospheric windows but are not defined by their opaque edges even at this low elevation site.

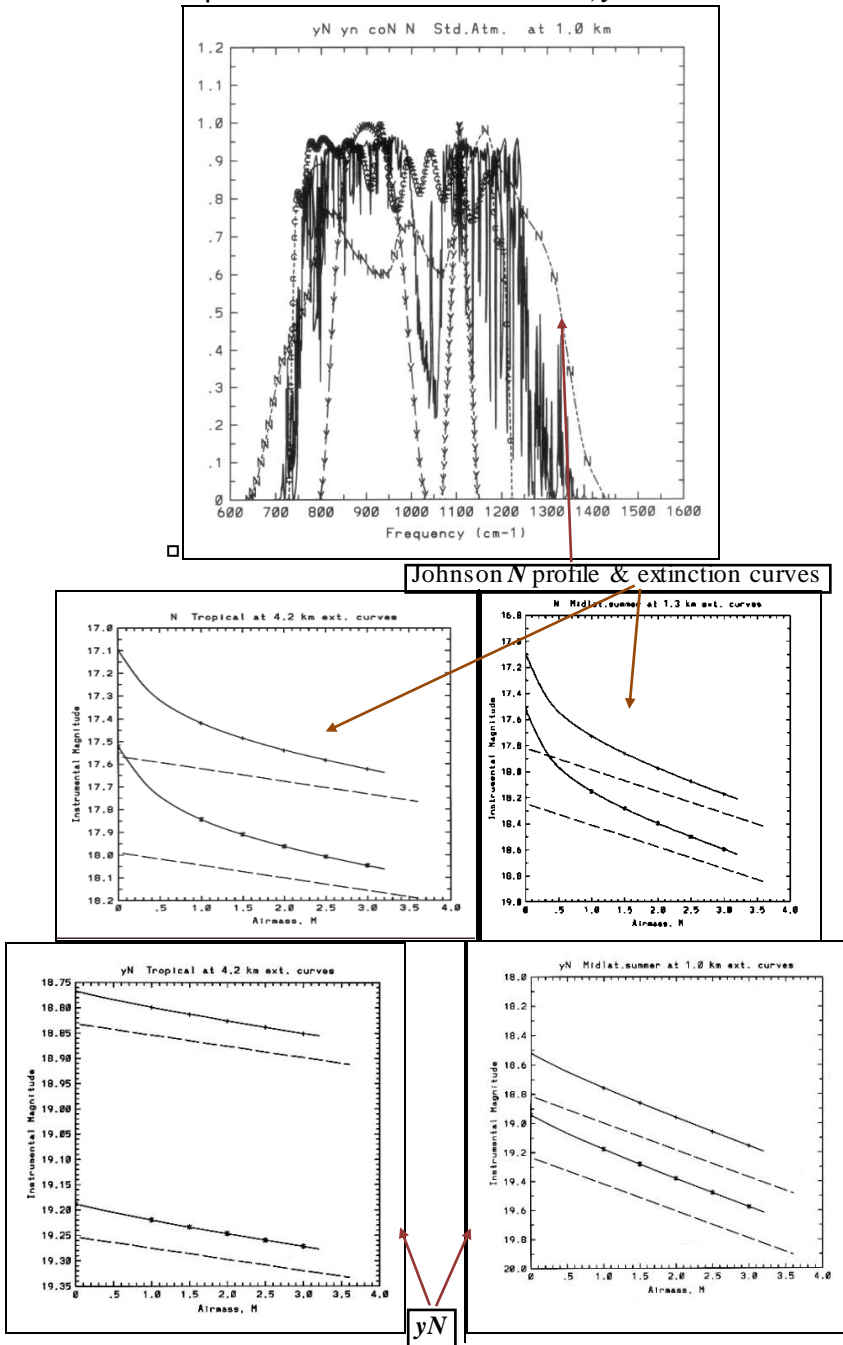
The  $10\mu\text{m}$  N window transmission and  $N$ ,  $yN$  extinction curves

Figure 10: The top plot shows the spectral transmission computed with MODTRAN for a standard atmosphere and a site at 1 km elevation above sea level for the N window spectral region. Superimposed on it are the profiles of two IRWG passbands, here designated  $yN$  and  $yn$  (temporary designations for the profiles presented in Young et al. (1994), and now referred to as  $iN$  and  $in$ , respectively. The original Johnson  $N$  passband, and a newer, somewhat improved one, designated  $coN$ . The lower four plots are simulated extinction curves for the  $N$  (top two), and the  $yN$  (bottom two) passbands. Plots on the left are computed for a tropical atmosphere and a site of 4.2 km; those on the right are computed for a mid-latitude, summer atmosphere at  $\sim 1$  km altitude. Note the decreased Forbes effect with the  $yN$  passband for both elevations, allowing thermal infrared photometry to be carried at many photometric sites.

## 5. Conclusion

We have followed parallel themes of the origins and development of the observation, modeling, and analysis of eclipsing variable star studies, and of the analytical tools and techniques to study them. We have explored the

progress in the field over the past century and with case studies highlighted the effects of improvements in data acquisition and quality as well as methods of analysis. Hopefully the exposition has shown that to study eclipsing binary stars is to undergo a journey of adventure and discovery. With space-scanning missions, we now have an

enormous collection of data, most of which will need to be followed up at ground-based observatories. For that work, we have the observing tools to produce the precise light & radial velocity curves and other observables needed for the analyses. With present modeling programs that incorporate physically realistic stellar and system models, the determination of ever more precise and accurate fundamental parameters of the component stars and the direction of their evolution seems secure. Henry Norris Russell's royal road even after more than a century of progress wide-open and inviting.

*Acknowledgements.* The author was honored and privileged to have been asked by Prof. I. Andronov to present a plenary paper on eclipsing binary stars at this important conference. I acknowledge with thanks the assistance of colleagues for some material in this presentation, particularly, R. E. Wilson, J. Kallrath, D. Terrell, and W. Van Hamme, and A. T. Young for insightful comments and corrections, but note that the views expressed are fully mine, and I alone bear responsibility for omissions or misrepresentations. Apologies to other colleagues, past and present, whose extensive and seminal works are not included in this personal and necessarily limited perspective. Most of my research drawn on here was funded by grants from the National Research Council and by the Natural Sciences and Engineering Research Council of Canada, the Research Grants Committee and the Department of Physics and Astronomy of the University of Calgary; specialized grants from agencies of the provincial government of Alberta, and the Cross Educational Foundation, all of which were received with gratitude.

#### Appendix: Objectives of Two IAU Commissions:

This work has undertaken a broad view of the subject through the perspective of a techniques astronomer, but the spirit of the undertaking is also in accord with that of at least two IAU Commissions. The scientific objectives and interests of Commission G1 – Binary and Multiple Stars ([https://iauarchive.eso.org/science/scientific\\_bodies/commissions/G1/](https://iauarchive.eso.org/science/scientific_bodies/commissions/G1/)) are:

- “the full range of observational tools that reveal binary and multiple systems (astrometry, photometry, spectroscopy, polarimetry, structure of cluster HR diagrams, products of space missions including Kepler, Gaia and LSST), and the interface of these with concerns of other Divisions and Commissions;
- kinematics, and ultimately dynamics, of binary and multiple systems;
- improved codes for binary and multiple systems, stellar atmospheres, structure and evolution, yielding surface compositions, tracks in the HR diagram, temporal changes in systemmasses and separations, etc;
- improvements of existing binary and multiple star system databases, regular production of publications (online and perhaps in print on paper), sharing databases, new codes, exciting discoveries, and

opportunities for interaction with other parts of the astronomical community; and

- accurate knowledge of the history of the subject and its continuing impact on astronomy in general.”

The statement of the scientific objectives of IAU Commission B6, Astronomical Photometry and Polarimetry ([https://iauarchive.eso.org/science/scientific\\_bodies/commissions/B6/](https://iauarchive.eso.org/science/scientific_bodies/commissions/B6/)) is:

“Commission B6 is concerned with photometric and polarimetric techniques and their standardization for the UV through far-IR/sub-mm spectral regions. These are essential tools in the exploration and investigation of astronomical objects and quantities.

Solutions to a wide range of scientific problems require calibrated photometry and polarimetry at better than the 1% level. Standardization is inescapable for exchanging data or merging data from different sources.”

#### References

- Adelman, S. J.: 2011, Optical Region Spectrophotometry: Past and Present, in *Astronomical Photometry: Past, Present, and Future*, eds. Milone, E. F. Sterken, C. (Springer, New York, Heidelberg, Dordrecht, London), 187-197.
- Apt, H.: 1995, *The AAS CD-ROM Series*, Vol. 5 (Oldsmar, FL: Advanced Data Solutions).
- Armbruster, C. W., Hull, A. B., Koch, R. H., Mitchell, R. J.: 2011, The Pierce-Blitzstein Photometer, in *Astronomical Photometry: Past, Present, and Future*, eds. Milone, E. F. Sterken, C. (Springer, New York, Heidelberg, Dordrecht, London), 83-105.
- Bailey, J., Cotton, D. V., De Horta, A., Kedziora-Chudczer, L., Shastri, O.: 2023, PICSARR: high-precision polarimetry using CMOS image sensors, *MNRAS*, arXiv:2301.09782 [astro-ph.IM]
- Bastien, P.: 2011, Measurement of Polarized Light in Astronomy, in *Astronomical Photometry: Past, Present, and Future*, eds. Milone, E. F. Sterken, C. (Springer, New York, Heidelberg, Dordrecht, London), 199-210.
- Berk, A., Bernstein, L. S., Robertson, D. C.: 1989, MODTRAN: A moderate Resolution Model for LOWTRAN 7, GL-TR-89-0122 (Air Force Geophysics Laboratory, Bedford, Mass.).
- Budaj, J., Richards, M. T.: 2004, A description of the shellspec code, *Contrib. Astron. Obs. Skalnaté Pleso*, 34, no. 3, 167-196.
- Budaj, J., Maliuk, A., Hubeny, I.: 2022, WD 1145+017: Alternative models of the atmosphere, dust clouds, and gas rings, *A&A*, 660, A72 [<https://doi.org/10.1051/0004-6361/202141924>]
- Cohen, M.: 2011, Absolute Photometry: Past and Present, in *Astronomical Photometry: Past, Present, and Future*, eds. Milone, E. F. Sterken, C. (Springer, New York, Heidelberg, Dordrecht, London), 177-186.
- Doppler, C.: 1842, Ueber das farbige Licht der Doppelsteme und einiger anderer Gestirne des Himmels, *Abhandlungen der Königl. Böhmischen Gesell. der Wissenschaften zu Prag*, V. Folge, Band ii, Prag, 465.
- Drilling, J. S., Landolt, A. U.: 2000, Normal Stars, Chapter 15, in A. N. Cox, *Allen's Astrophysical Quantities*, (AIP Press Springer-Verlag, New York), Table 15.6, p. 387.

- El-Badry, K.: 2024, Gaia's binary star renaissance, *New Astronomy Reviews*, **98**, 6.
- Gorda, S. Yu.: 2016, Radial Velocity of the Spectroscopic Binary HD 25639 (ADS 2984A), *Astron. Lett.*, **42**, 693-702.
- Hall, J. S.: 1934, Photo-electric Photometry in the Infrared with the Loomis Telescope, *ApJ*, **79**, 145-181.
- Hardie, R. H.: 1962, Photoelectric Reductions, Chapter 8, in *Astronomical Techniques*, ed. W. A. Hiltner, (The University of Chicago Press, Chicago), 178-208.
- Herschel, W.: 1803, XV. Account of the Changes that have happened, during the last Twenty-five Years, in the relative Situation of Double-Stars; with an Investigation of the Cause to which they are owing, *Phil. Trans. Roy. Soc.*, **93**, 339-382 + Plates VII and VIII.
- Huggins, W.: 1868, Further observations on the spectra of some of the stars and nebulae, with an attempt to determine therefrom whether these bodies are moving towards or from the Earth, also observations on the spectra of the Sun and of Comet II, *Phil. Trans. Roy. Soc.*, **158**, 529-564.
- Johnson, H. L.: 1964, *Bol. Tonantzinla Tacubaya*, **3**, 305-324.
- Johnson, H. L.: 1966: Astronomical Measurements in the Infrared, in *Ann. Rev. A&Aph*, **4**, 193-206.
- Kallrath, J.: 2022, Fifty Years of Eclipsing Binary Analysis with the Wilson-Devinney Model, *Galaxies*, **10**, 17-30.
- Kallrath, J., Milone, E. F.: 2009, *Eclipsing Binary Stars: Modeling & Analysis*, 2nd ed. (Springer, New York, Dordrecht, Heidelberg, London).
- Kallrath, J.; Milone, E.F.; Terrell, D.; Young, A.T.: 1998, Recent Improvements to a Version of the Wilson-Devinney Program. *Astrophys. J.*, **508**, 308-313
- Kopal, Z.: 1950, The Computation of Elements of Eclipsing Binary Systems. Harvard Observatory Monograph No. 8.
- Kopal, Z.: 1959, *Close Binary Systems*. (John Wiley & Sons, New York), 127.
- Kopal, Z., Shapley, M. B.: 1956, Catalogue of the Elements of Eclipsing Binary Systems, Reprint, Jodrell Bank Annals, 1, fascicle. 4, 168-169.
- Kostov, V. B., Powell, B. P., Fornear, A. U. et al.: 2025, The TESS Ten Thousand Catalog: 10,001 Uniformly Vetted and Validated Eclipsing Binary Stars Detected in Full-frame Image Data by Machine Learning and Analyzed by Citizen Scientists, *ApJS*, **279**, 50 (32pp).
- Kurpinska-Winiarska, M., Oblak, E., Winiarski, M., Kundera, T.: 2000, Observations of Two Hipparcos Eclipsing Variables IBVS, **49**, No. 4823, 1 -3.
- Lagrange, J.-L.: 1772, *Essai d'une nouvelle méthode pour résoudre le problème des trois corps*. Oeuvres complètes VI, Prix de l'Academie royale des sciences de Paris, tome IX, 229-331.
- Landolt, A. U.: 1983, UBVRI Photometric Standard Stars around the Celestial Equator, *AJ*, **88**, 439-460.
- Leavitt, H. S. & Pickering, E. C.: 1917, The North Polar Sequence, *Harvard Annals*, **71**, No. 3, 47-232.
- Li, X.-Z., Zhu, Q.-F., Ding, X. et al.: 2024, Physical Parameters of 11,100 Short-period ASAS-SN Eclipsing Contact Binaries, *ApJS*, **271**, 32 (9pp).
- Lucy, L B.: 1968, The Light Curves of W Ursae Majoris, *ApJ*, **153**, 877-884.
- Marigo, P., Girardi, L., Bressan, A., Groenewegen, M. A. T., Silva, L.,& Granto, G. L.: 2008, Evolution of asymptotic giant branch stars. II. Optical to far-infrared isochrones with improved TP-AGB models, *A&A*, **482**, 883-905.
- Mayor, M., Queloz, D.: 1995, A Jupiter-mass Companion to a Solar-type Star, *Nature*, **378**, 355-359.
- Michell, J.: 1767, An Inquiry into the Probable Parallax, and Magnitude of the Fixed Stars, from the Quantity of Light Which They Afford us, and the Particular Circumstances of Their Situation, *Phil. Trans. Roy. Soc.*, **57**, 234-264.
- Milone, E. F., ed.: 1989, Infrared Extinction and Standardization, *Lect. Not. in Phys.*, **341** (Springer-Verlag, Berlin, Heidelberg).
- Milone, E. F.: 2003, Fundamental stellar parameters from eclipsing binaries, in *GAIA, Spectroscopy, Science and Technology*, ed. U. Munari, ASP Conf. No. 298, 303-312.
- Milone, E. F., Kallrath, J.: 2008, The Tools of the Trade and the Products they Produce: Modeling of Eclipsing Binary Observables, in *Short-Period Binary Stars: Observations, Analysis, and Results*, eds. Milone, E.F., Leahy, D.A., Hobill, D.W. (Springer Science+Business Media B.V.), 191-214.
- Milone, E.F., Pel, J. W.: 2011, High Road to Astronomical Photometric Precision: Differential Photometry in Astronomical Photometry: Past, Present, and Future, eds. Milone, E. F., Sterken, C. (Springer, New York, Dordrecht, Heidelberg, London), pp 33-68.
- Milone, E. F., Sterken, C., eds.: 2011, *Astronomical Photometry: Past, Present, and Future*, (Springer, New York, Dordrecht, Heidelberg, London).
- Milone, E. F., Young, A. T.: 2005, An Improved IR Passband System for Ground-Based Photometry: Realization, *PASP*, **117**, 485-502.
- Milone, E. F., Young, A. T.: 2007, Standardization and the Enhancement of Infrared Precision, in *The Future of Photometric, Spectrophotometric, and Polarimetric Standardization*, ed. C. Sterken, ASP Conf. Series 999, 387-407.
- Milone, E.F., Young, A.T.: 2011, The Rise and Improvement of Infrared Photometry, in *Astronomical Photometry: Past, Present, and Future*, eds. Milone, E.F., Sterken, C. (Springer, New York, Dordrecht, Heidelberg, London), pp 125-141.
- Milone, E. F., Kurpinska-Winiarska, M., Oblak, E.: 2010, Observations and Analysis of the Eccentric Orbit Eclipsing Binary HP Draconis, *AJ*, **140**, 129-137.
- Milone, E. F., Wilson, R. E., and Hrivnak, B. J.: 1987, RW Comae Berenices III. Light Curve Solution and Absolute Parameters, *ApJ*, **318**, 325-338.
- Mishra, A. K., Kamath, U. S.: 2022, Filters for NIR astronomical photometry: comparison of commercial IRWG filters and design using OpenFilters, *Journal of Astrophysics and Astronomy*, **43**, 13 (16pp).
- Mishra, A. K., Sarkar, D. R., Prajapati, P., Singh, A., Kasarla, P. K., Ganesh, S.: 2024, A summary of instruments proposed for observing pulsating variables from the Mt. Abu Observatory, *Journal of Astrophysics and Astronomy*, **45(2)**, 34 (15pp).
- Mowlavi, N. et al.: 2023, Gaia Data Release 3: The First Gaia catalogue of eclipsing-binary candidates, *A&A*, **674**, A16 (45pp).
- Nelson, R. H., Terrell, D., Milone, E. F.: 2023, A Critical Review of Period Analyses and Implications for Mass Exchange in W UMa Eclipsing Binaries: Paper 4, *New Astronomy Reviews*, 97. [\[https://doi.org/10.1016/j.newar.2023.101684\]](https://doi.org/10.1016/j.newar.2023.101684)
- Nelson, R. H., Milone, E. F., Van Leeuwen, J., Terrell, D., Penfield, J. E., Kallrath, J.: 1995, *AJ*, **110**, 2400-2407.
- Pickering, E. C.: 1880, Dimensions of the Fixed Stars with especial Reference to Binaries and Variables of the Algol Type, *Proceedings of the American Academy of Arts and Sciences*, **16**, 1.
- Piotrowski, S. L.: 1948, Some Remarks on the Weights of Unknowns as Determined by the Methods of Differential Corrections, *Procs., Nat. Acad. Scis.*, **34**, No. 2, 23-26.

- Plavec, M. J.: 1980, IUE Observations of Long Period Eclipsing Binaries: A Study of Accretion onto Non-degenerate Stars, in *Close Binary Stars: Observations and Interpretation*, eds. M. J. Plavec, D. M. Popper, R. K. Ulrich. IAU Symposium 88, 251-261.
- Plavec, M., Koch, R. H.: 1978, Detection of Emission Lines of Hot Plasma in Five Peculiar Eclipsing Binary Systems, IBVS, Vol. 15, No. 1482, 1-3.
- Pogson, N.: 1856, Magnitudes of Thirty-six of the Minor Planets for the First Day of Each Month of the Year 1857, *MNRAS*, **17**, 12-16.
- Prša, A.: 2018, *Modeling and Analysis of Eclipsing Binary Stars*; IOP Publishing: Bristol, UK, pp. 2514-3433.
- Prša, A., Kochoska, A., Conroy, K. E. et. Al.: 2022, TESS Eclipsing Binary Stars. I. Short-cadence Observations of 4584 Eclipsing Binaries in Sectors 1-26, *ApJS*, **258**, 16 (22pp).
- Roche, E. A.: 1849, *La Figure d'une Masse Fluide Soumise à l'Attraction d'un Point Éloigné (I)*, Acad, des Sciences et Lettres de Montpellier, Mém, de la Section des Sciences, Tome Premier (1847-1850), 243-262.
- Roche, E. A.: 1850, *La Figure d'une Masse Fluide Soumise à l'Attraction d'un Point Éloigné (II)*, Acad, des Sciences et Lettres de Montpellier, Mém, de la Section des Sciences, Tome Premier (1847-1850), 333-348.
- Russell, H.N.: 1912a, On the Determination of the Elements of Eclipsing Variable Stars I, *ApJ*, **35**, 315-340.
- Russell, H.N.: 1912b, On the Determination of the Elements of Eclipsing Variable Stars II, *ApJ*, **36**, 54-74.
- Russell, H. N.: 1948, The Royal Road of Eclipses (First Henry Norris Russell Lecture), in *Centennial Symposia, Contributions on Interstellar Matter, Electronic and Computational Devices, Eclipsing Binaries, The Gaseous Envelope of the Earth*. Cambridge, MA, Harvard Observatory Monograph, 7, 181-209.
- Russell, H. N. & Merrill, J. E.: 1952, The Determination of the Elements of Eclipsing Binaries. Contr. Princeton Univ. Obs, No. 26. (The Observatory, Princeton, N.J.)
- Russell, H. N. & Shapley, H.: 1912a, On the Darkening of the Limb in Eclipsing Variable Stars I, *ApJ*, **36**, 239-254.
- Russell, H. N. & Shapley, H.: 1912b, On the Darkening of the Limb in Eclipsing Variable Stars II, *ApJ*, **36**, 385-408.
- Sahman, D. I., Dhillon, V. S., Marsh, T. R., et al: 2013, CI Aql a Type Ia supernova progenitor? *MNRAS*, **433**, 1588-1598.
- Schaefer, B. E.: 2011, The Change of Orbital Periods across Eruptions and the Ejected Mass for Recurrent Novae CI Aquilae and U Scorpii, *ApJ*, **742**, 112 (28pp).
- Schaefer, B. E.: 2014, Erratum: "The Change of Orbital Periods across Eruptions and the Ejected Mass for Recurrent Novae CI Aquilae and U Scorpii" (2011, *ApJ*, 742, 112), *ApJ*, **781**, 127.
- Schilt, J.: 1922, A Thermo-electric Method of Measuring Photographic Magnitudes, *Bulletin of the Astronomical Institutes of the Netherlands*, 1, No. 10, 51-52.
- Southworth, J.: 2025, Rediscussion of Eclipsing Binaries. Paper XXVI. The F-Type Long-Period System HP Draconis. [arXiv:2508.04218v1 [astro-ph.SR] 6 Aug 2025]
- Stefanik, R. P., Latham, D. W., & Torres, G.: 1999, Radial-Velocity Standard Stars, in Hearnshaw, J. B. & Scarfe, C. D., eds., *Precise Stellar Radial Velocities*, IAU Colloquium 170, *ASP Conf. Ser.*, **185**, 354-366.
- Sterken, C., Milone, E. F., and Young, A. T.: 2011, Photometric Precision and Accuracy, in *Astronomical Photometry: Past, Present, and Future*, eds. Milone, E. F. Sterken, C. (Springer, New York, Heidelberg, Dordrecht, London), *ASSL*, 373, 1-32.
- Stetson, H. T.: 1916, On an Apparatus and Method for Thermo-Electric Measurements in Photographic Photometry. I. *Astron. J.*, **43**, 253-285.
- Stetson, H. T.: 1916, On an Apparatus and Method for Thermo-Electric Measurements in Photographic Photometry. II. Application to Variable Stars. *Astron. J.*, **43**, 325-340.
- Tamajo, E., Munari, U., Siviero, A., Tomasella, L., Dallaporta, S.: 2012, *A&A*, **539**, A139.
- Terrell, D.: 2025, This summer's Variable Star of the Season. Available at: ([https://www.aavso.org/vsots\\_betalyr](https://www.aavso.org/vsots_betalyr)).
- Tokovinin, A.: 2025, Spectroscopic Orbits of Subsystems in Multiple Stars, XI, *AJ*, **170**, 143. [doi.org/10.3847/1538-3881/adee23].
- Tulenius, A.: 1740, *Dissertatio astronomica de constellatione Arietis (Homiae, Stockholm)Vogel, H. C.: 1890, Spectrographische Beobachtungen an Algol, AN*, **123**, 289-292.
- Walraven, T.: 1953, On the Use of Servomechanisms in the Photometry of Stars, in *Astronomical Photoelectric Photometry*, ed. Wood, F. B. Publications, AAAS, 114.
- Wesselink, A. J.: 1941, A Study of SZ Camelopardalis. *Leiden Annalen*, 17, Part 3.
- Whitford, A. E.: 1932, The Application of a Thermionic Amplifier to the Photometry of Stars, *ApJ*, **76**, 213-223.
- Whitford, A. E., Kron, G. E.: 1937, Photoelectric Guiding of Astronomical Telescopes, *The Review of Scientific Instruments*, 8, 78-82.
- Williams, M. D., and Milone, E. F.: 2013, Results from the Rothney Astrophysical Observatory Variable Star Search Program: Background, Procedure, and Results from RAO Field 1, *Journal of Astronomical Data*, 19 (2), 1-86. [arxiv.org/abs/1101.5650]
- Wilson, R. E.: 1971, A Model of Epsilon Aurigae, *ApJ*, **170**, 529-539.
- Wilson, R. E.: 1979, Eccentric Orbit Generalization and Simultaneous Solution of Binary Star Light and Velocity Curves, *ApJ*, **234**, 1054-1066.
- Wilson, R. E.: 1981, Equilibrium Figures for beta Lyrae Type Disks, *ApJ*, **251**, 246-258.
- Wilson, R. E.: 1990, Accuracy and Efficiency in the Binary Star Reflection Effect, *ApJ*, **356**, 613-622.
- Wilson, R. E.: 2018, Self-gravitating Semi-transparent Circumstellar Disks: An Analytic Model, *ApJ*, **869**, 19-37.
- Wilson, R. E. & Devinney, E. J.: 1971, Realization of Accurate Close-Binary Light Curves: Application to MR Cygni, *ApJ*, **166**, 605-619.
- Wilson, R. E., Honeycutt, R. K.: 2014, Outburst-related Period Changes of Recurrent Nova CI Aquilae, *ApJ*, **795**, 8 (6pp).
- Wilson, R. E., Van Hamme, W.: 2025, An Equipotential Disk Model with Irradiation for Nova-Like Variables, *ApJ*, in press.
- Wing, R. F.: 2011, On the Use of Photometry in Spectral Classification, in *Astronomical Photometry: Past, Present, and Future*, eds. Milone, E. F., Sterken, C. (Springer, New York, Dordrecht, Heidelberg, London), pp 143-176.
- Yang, S.-C., Han, W.-B., Tagawa, H., Li, S., Zhang, C.: 2025, Indication for a Compact Object Next to a LIGO-Virgo Binary Black Hole Merger, *ApJL*, **988**, No. 2, L41(9pp).
- Young, A. T., Milone, E. F., Stagg, C. R.: 1993, On Improving IR Photometric Passbands, in *Stellar Photometry – Current Techniques and Future Developments*, eds, C. J. Butler, I. Elliott (University Press, Cambridge), 235-241.
- Young, A. T., Milone, E. F., Stagg, C. R.: 1994, On Improving IR Photometric Passbands, *A&AS*, **105**, 259-279.